ZEITLICHE VARIATIONEN DES ERDSCHWERFELDES AUS SATELLITENBEOBACHTUNGEN

Kann die Lücke zwischen GRACE und GFO geschlossen werden?

Matthias Weigelt

GRACE und GRACE Follow-On (GFO)

Low-low

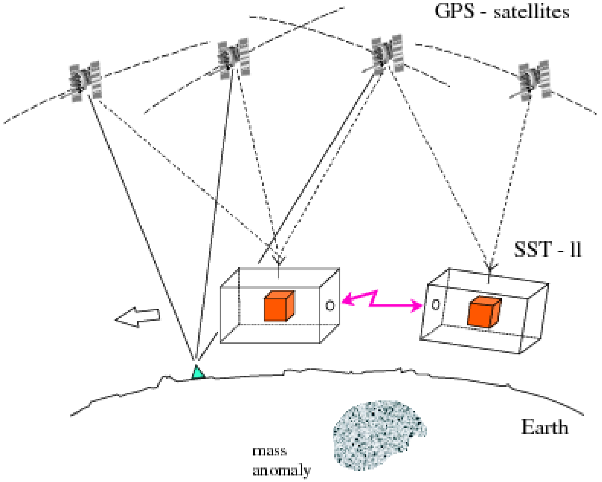

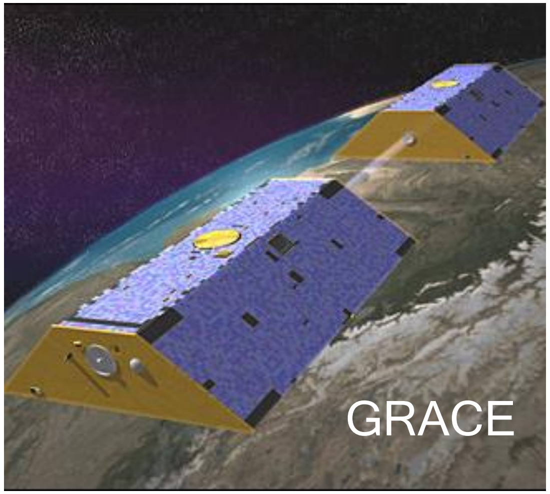

© CSR Texas

- K-Band (Laser)
- GPS
- Accelerometer

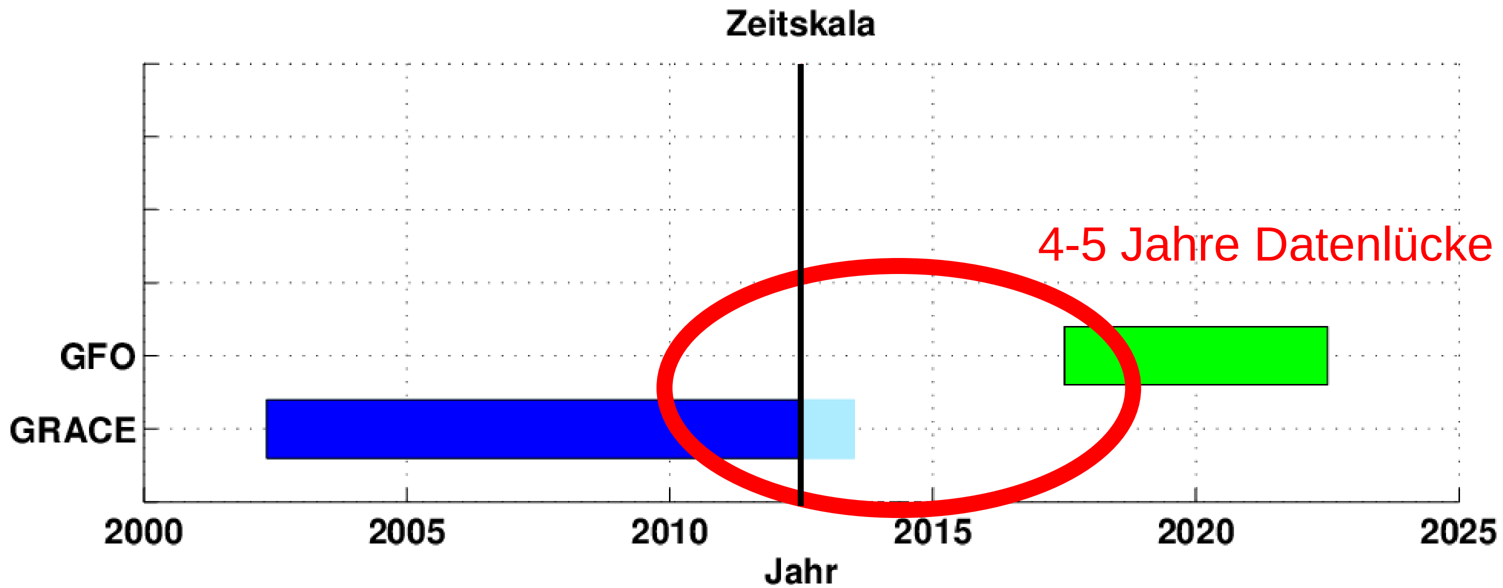

High-low

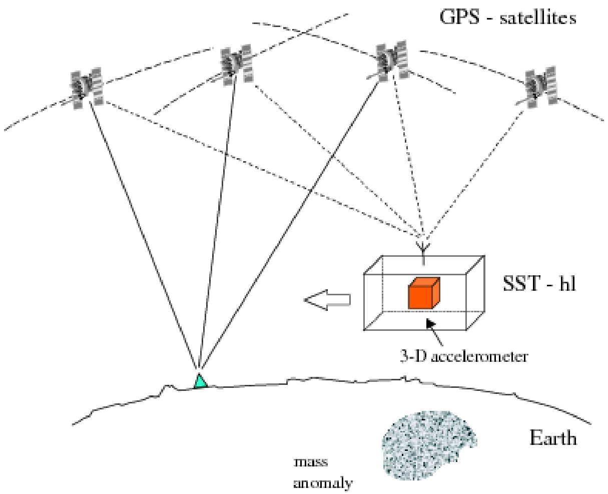

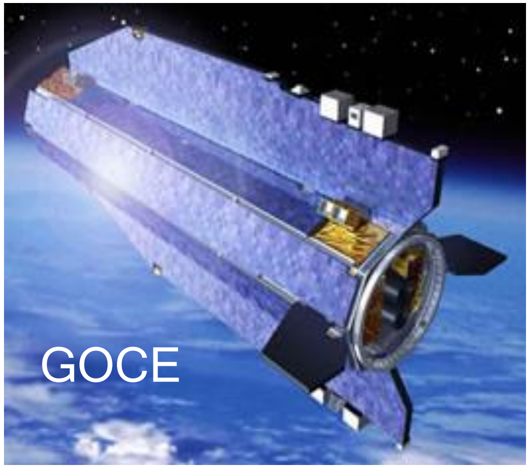

© ESA

© EADS Astrium

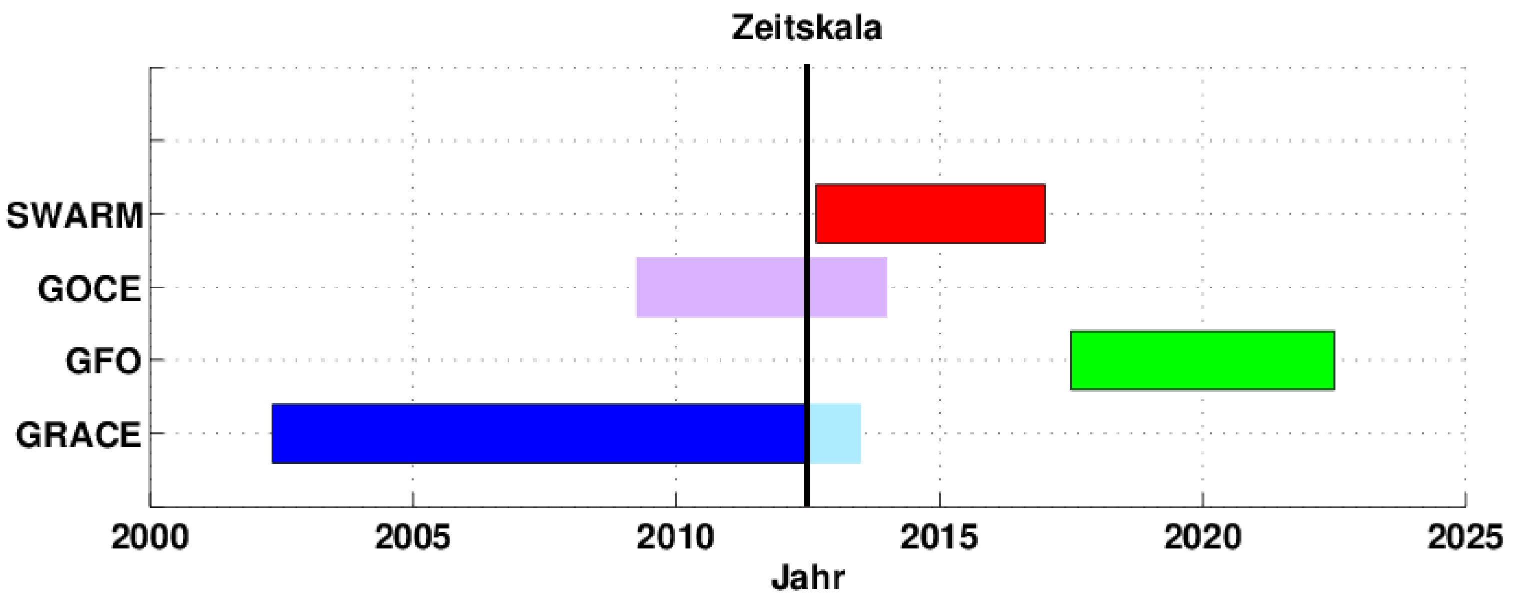

METHODIK AM BEISPIEL CHAMP

Beschleunigungsansatz:

$$\nabla V = \ddot{\vec{x}} - \vec{f}_{\text{3rdBody}} - \vec{f}_{\text{Tides}} - \vec{f}_{\text{Rel}} - \vec{f}_{\text{Grav}}$$

$$V = \frac{GM}{R} \sum_{l=0}^{\infty} \left(\frac{R}{r}\right)^{l+1} \sum_{m=0}^{l} \bar{P}_{lm}(\sin\phi)\left(\bar{C}_{lm}\cos m\lambda + \bar{S}_{lm}\sin m\lambda\right)$$

mit	GM	Gravitationskonstante mal Erdmasse
	R	Radius der Erde
	r, ϕ, λ	sphärische Koordinaten des Berechnungspunktes
	$\bar{P}_{lm}$	Legendre-Funktion
	l, m	Grad, Ordnung
	$\bar{C}_{lm}, \bar{S}_{lm}$	(unbekannte) Kugelfunktionskoeffizienten

Spektrale Darstellung

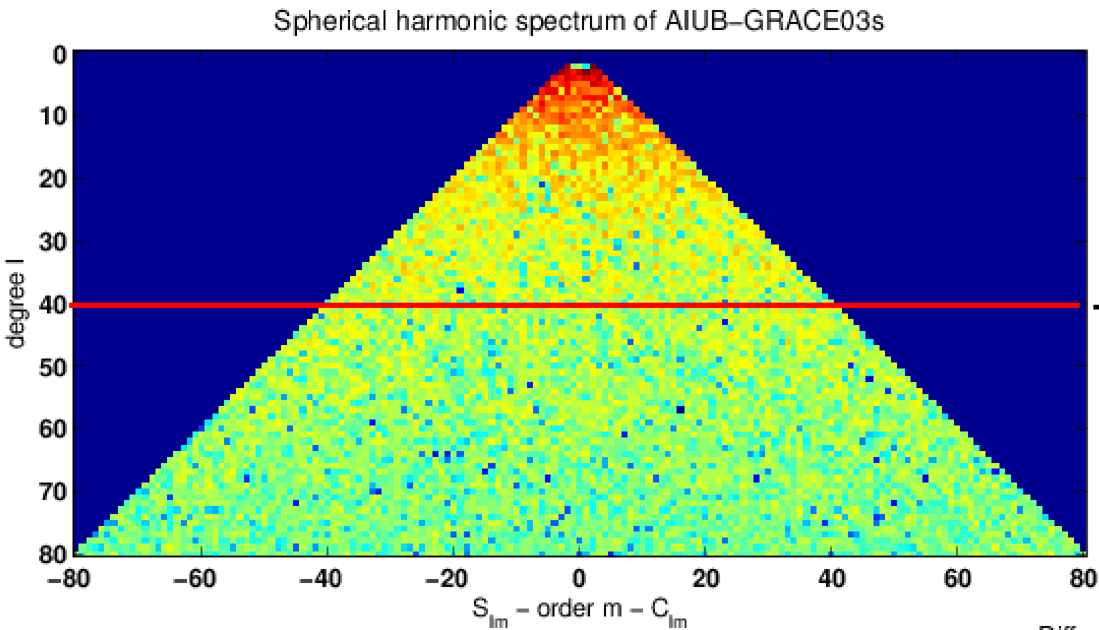

$$c_n = \sqrt{\frac{1}{2n+1}\sum_{m=0}^{n} \bar{C}_{nm}^2 + \bar{S}_{nm}^2}$$

Grad-RMS entspricht der mittleren Signal-/Fehlerstärke pro Grad

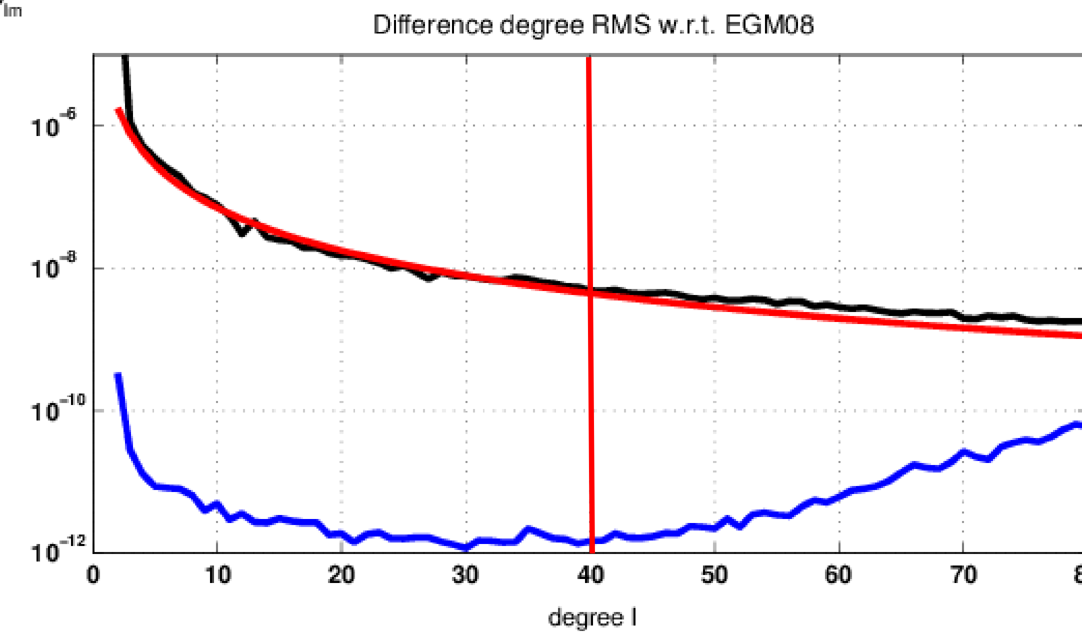

MONATSLÖSUNGEN

CHAMP state of the art

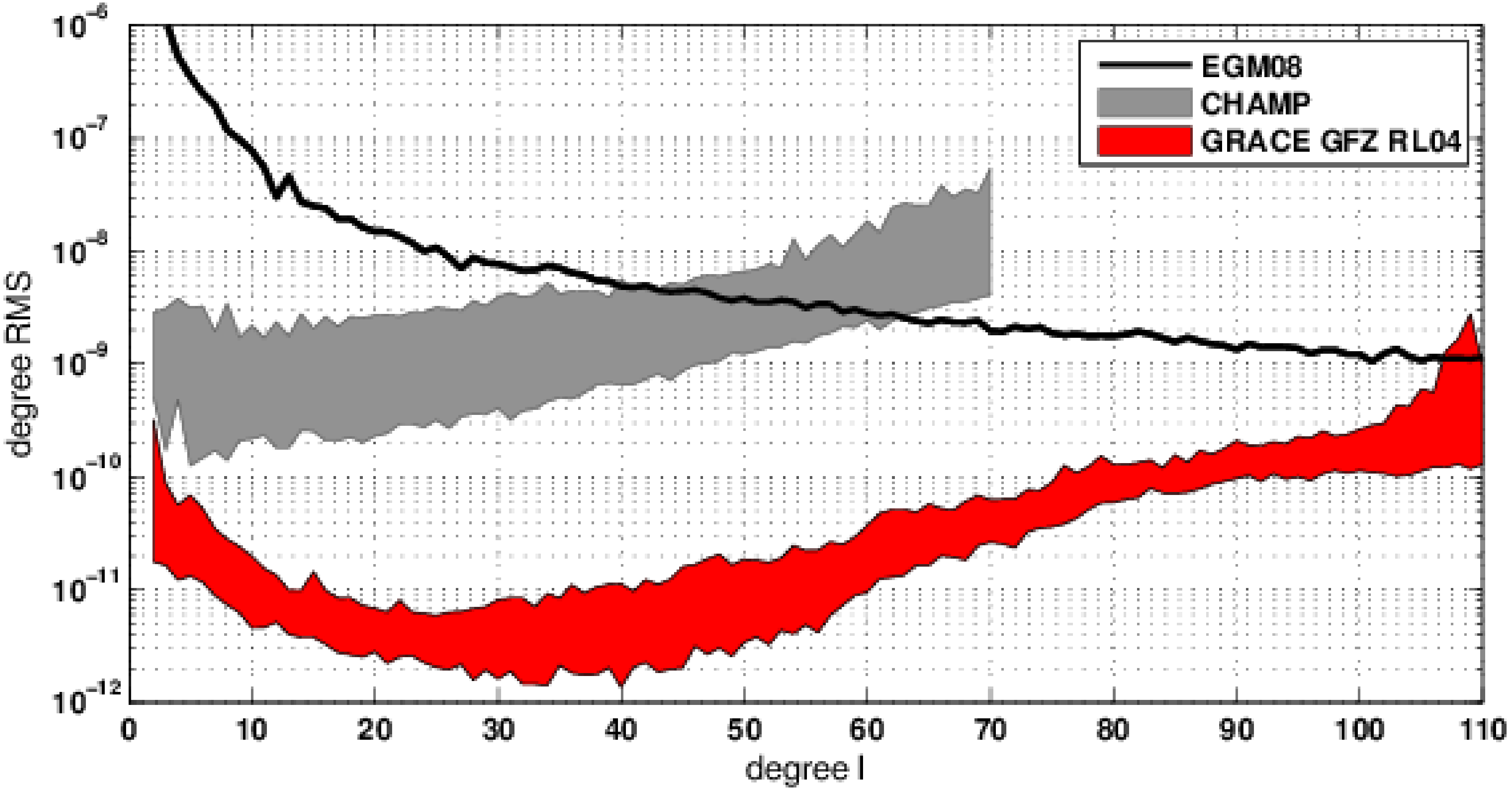

GPS - Positionen: AIUB

- Messwerte alle 10 s
- Schätzung eines Models fürs absolute Antennenphasenzentrum
- neue IGS Standards
- …

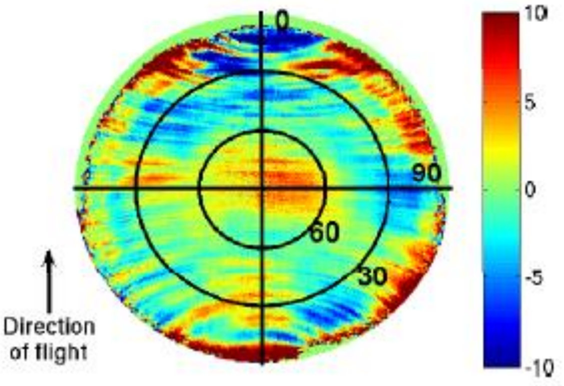

Prange 2010

Hintergrundmodelle:

- JPL ephemeris DE405
- Solid Earth tides (IERS conventions)
- Solid Earth pole tides (IERS conventions)
- Ocean tides (FES 2004)
- Ocean pole tides (IERS conventions, Desai 2002)
- Atmospheric tides (N1-model, Biancale and Bode 2006)
- Relativistic corrections (IERS conventions)
- AOD1B-product (Flechtner 2008)

CHAMP Monatslösungen

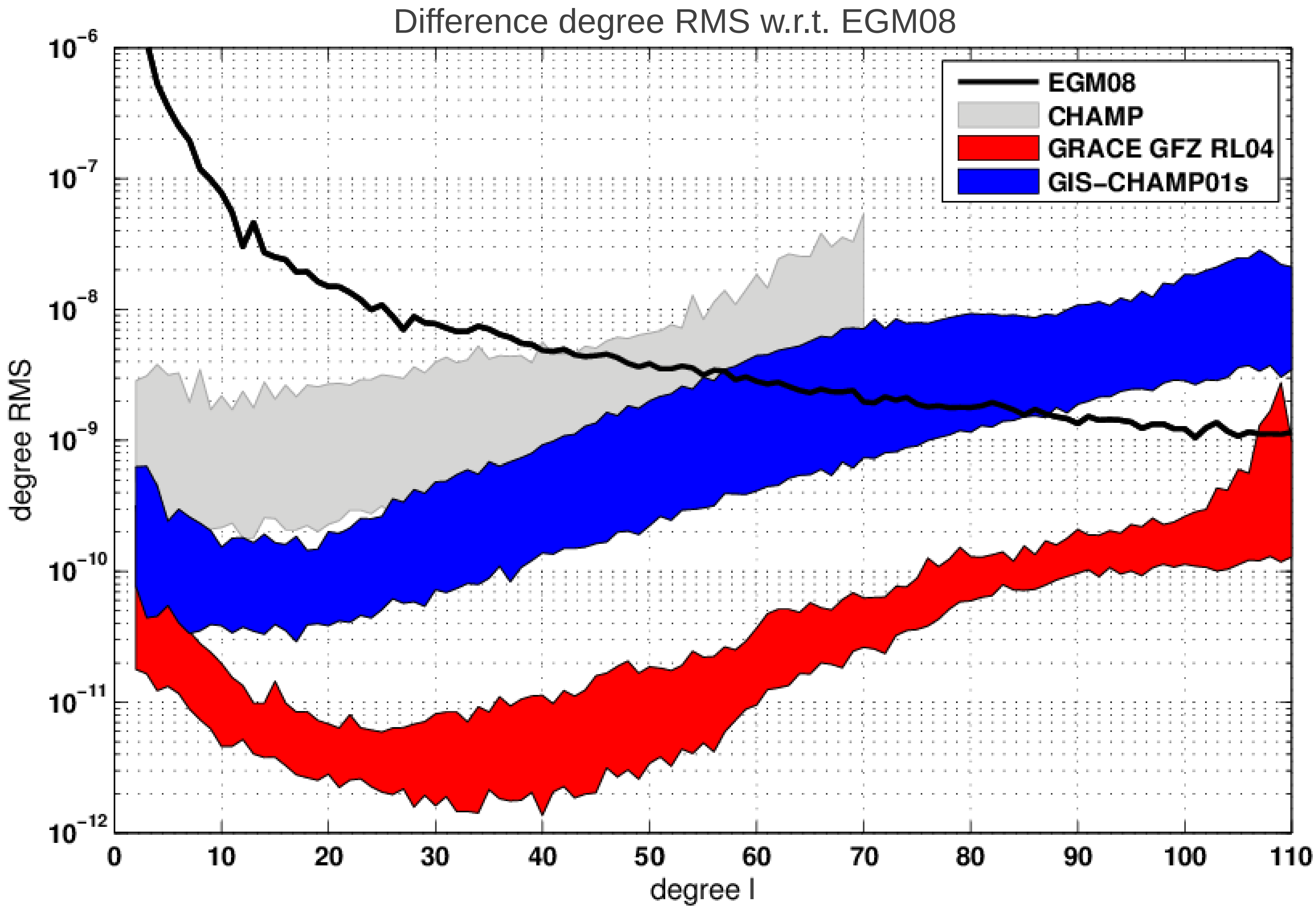

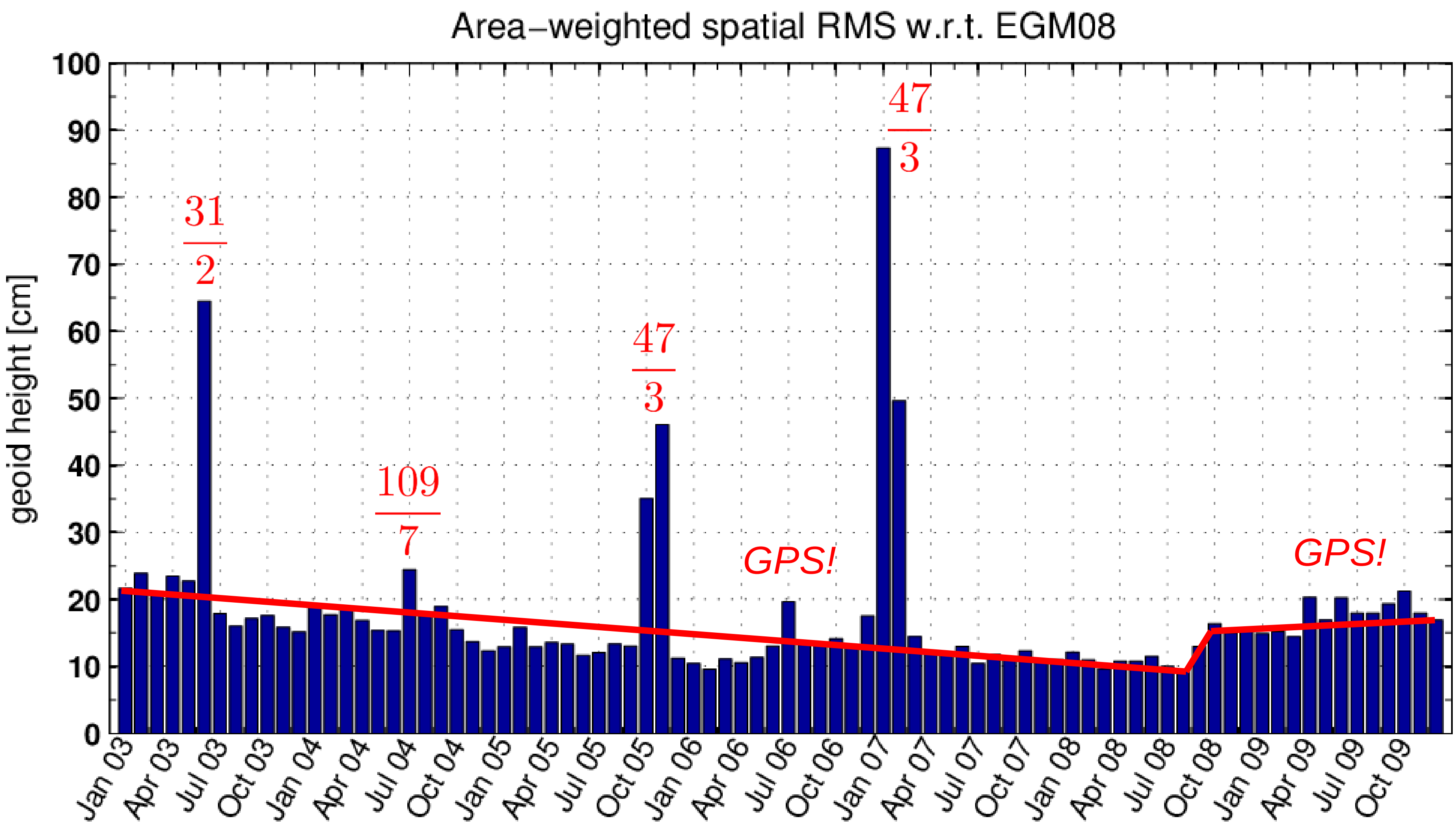
Area–weighted spatial RMS w.r.t. EGM08
geoid height [cm]
100
90
80
70
60
50
40
30
20
10
0
31/2
109/7
47/3
47/3
GPS!
GPS!
Jan 03
Apr 03
Jul 03
Oct 03
Jan 04
Apr 04
Jul 04
Oct 04
Jan 05
Apr 05
Jul 05
Oct 05
Jan 06
Apr 06
Jul 06
Oct 06
Jan 07
Apr 07
Jul 07
Oct 07
Jan 08
Apr 08
Jul 08
Oct 08
Jan 09
Apr 09
Jul 09
Oct 09

CHAMP Monatslösungen

Time series of SH-coefficients: GRACE vs. CHAMP (annual) – scaled by 10^{10}

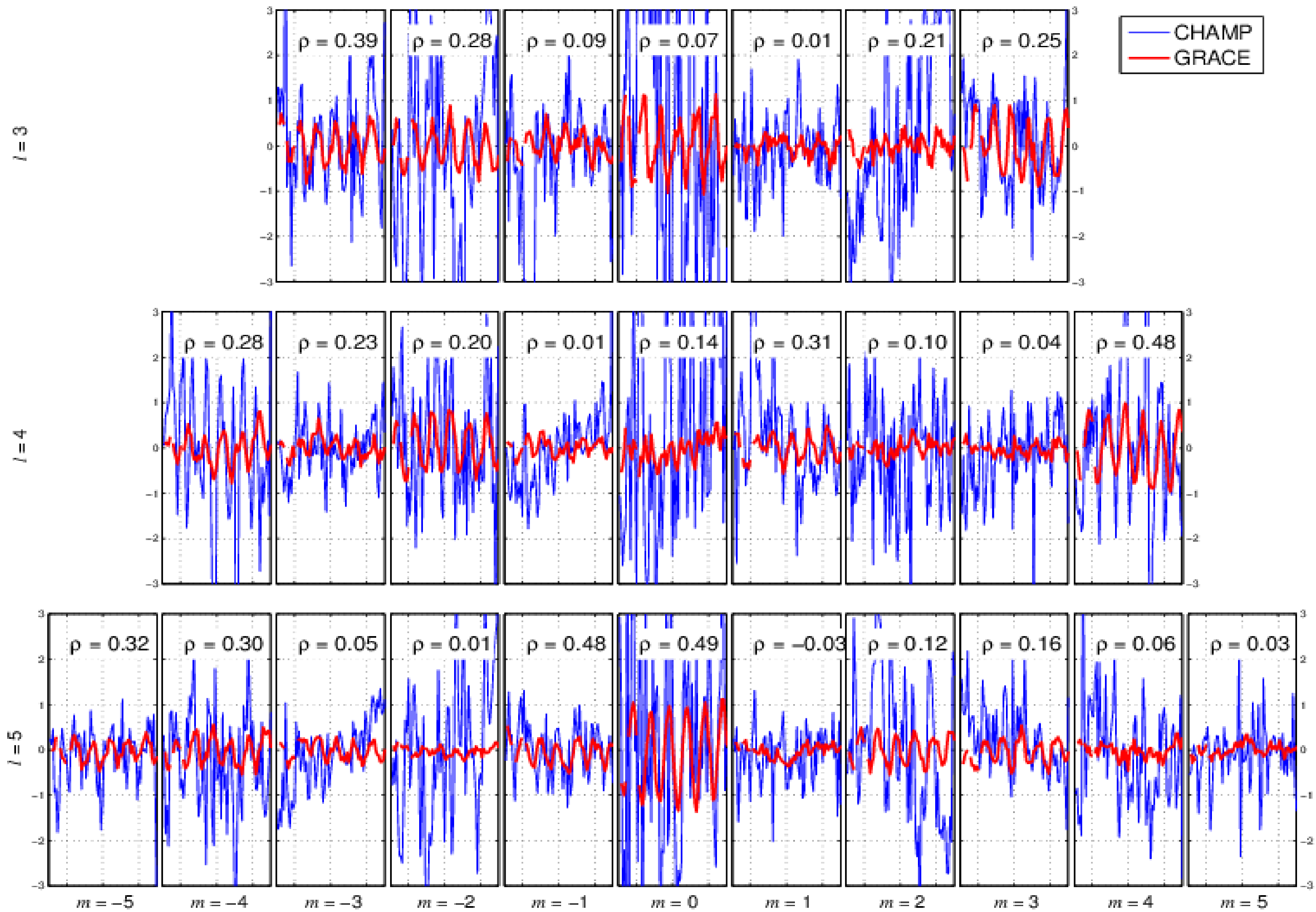

MODELLIERUNG

Modellierung der Zeitvariabilität

$$\bar{C}(t) = \bar{C}_0 + \dot{\bar{C}}\,t + \sum_{n=1}^{N} \bar{C}_n^{\cos} \cos(\omega_n t) + \bar{C}_n^{\sin} \sin(\omega_n t)$$

$$\bar{S}(t) = \bar{S}_0 + \dot{\bar{S}}\,t + \sum_{n=1}^{N} \bar{S}_n^{\cos} \cos(\omega_n t) + \bar{S}_n^{\sin} \sin(\omega_n t)$$

- Pro:
  - einfach
  - Korrelationen zwischen Koeffizienten
- Con:
  - mittlere Zeitvariabilität der Messperiode
  - Frequenzen unbekannt
  - Variationen der Frequenzen nicht möglich

Zeitreihe der Koeffizienten

Time series of SH-coefficients: GRACE vs. CHAMP (annual) – scaled by 10^{10}

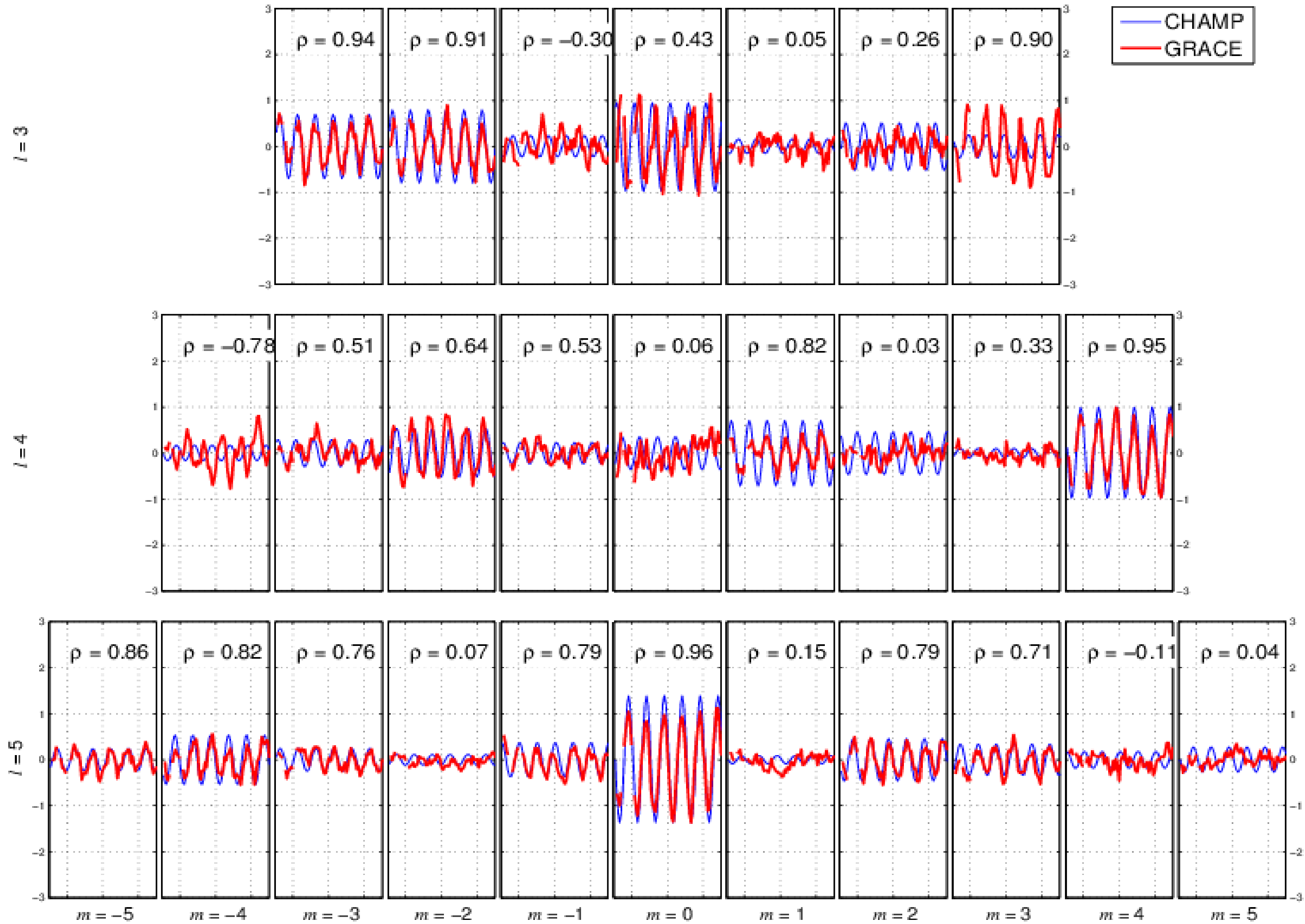

Grad RMS der Monatslösungen

$$L_{Max} = 110$$
$$L_{Max}^{TV} = 8$$

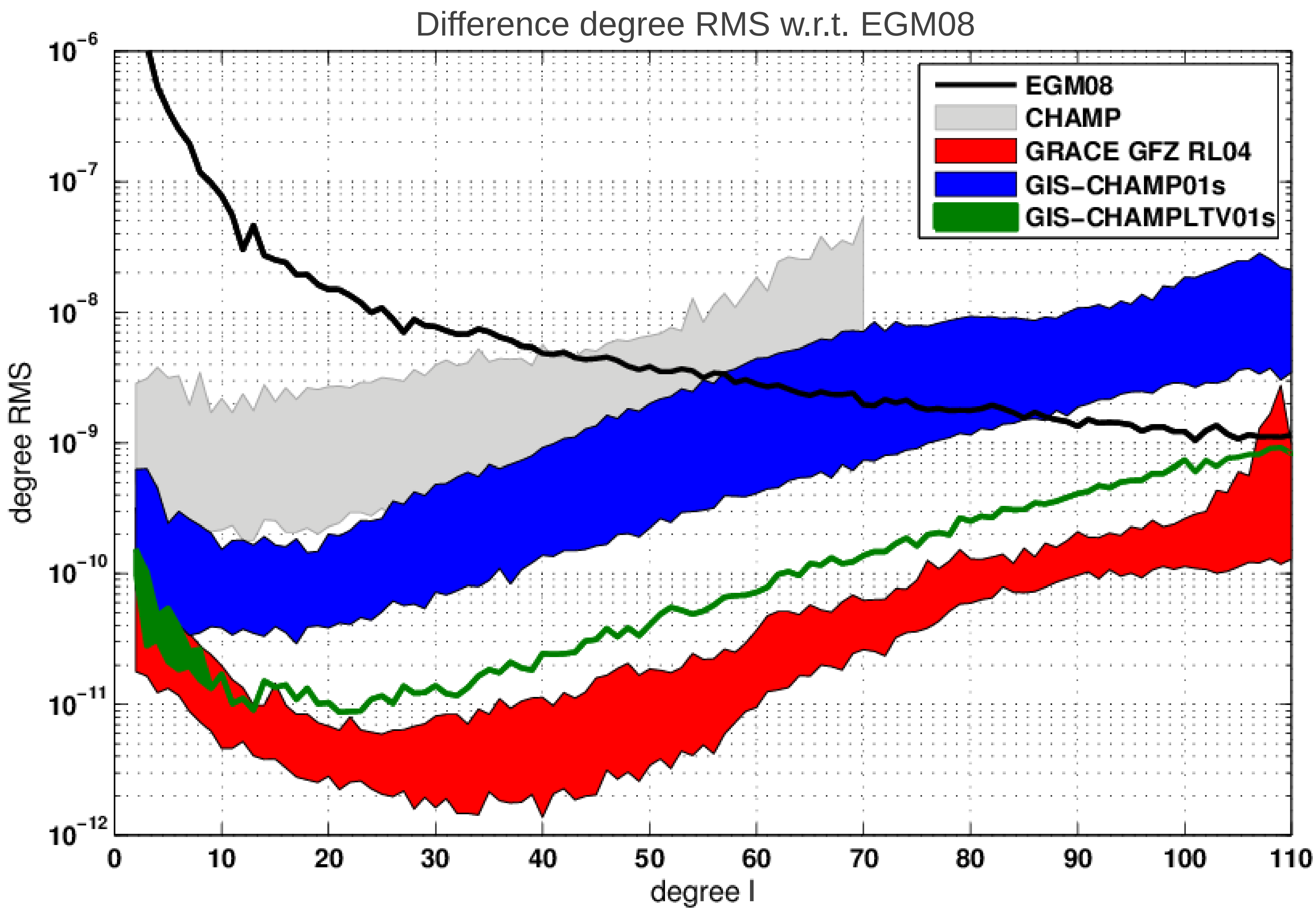

Beispiel: Zeitreihe von S_{22}

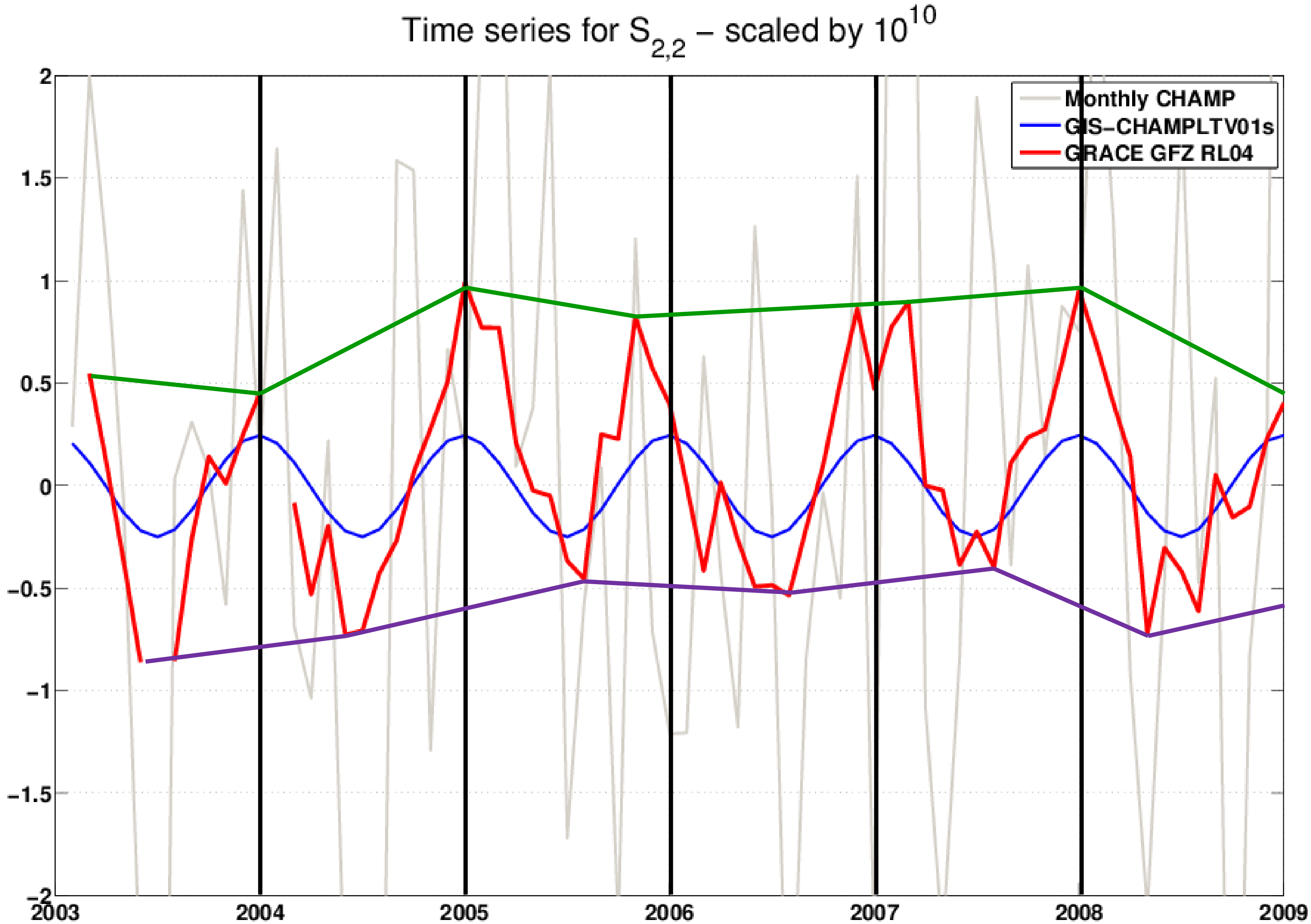

KALMAN FILTER

Filteransatz

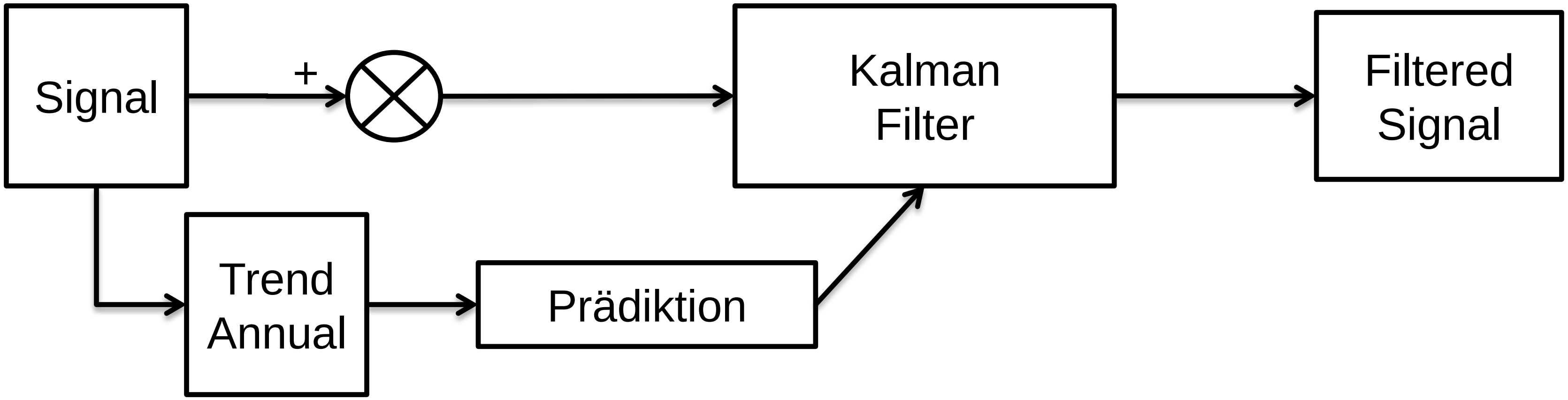

- Pro:
  - Anwendung auf die Zeitreihen der Koeffizienten (einfache Umsetzung)
  - Variationen von Amplitude und Phase möglich
- Con:
  - Ausreißersuche für Prädiktionsmodell
  - Vernachlässigung der Korrelationen zwischen Koeffizienten
  - Verlust der Redundanz

Filtered monthly gravity field solutions (3/6)

Time series of SH-coefficients: GRACE vs. High-Low (filtered) – scaled by 10^{10}

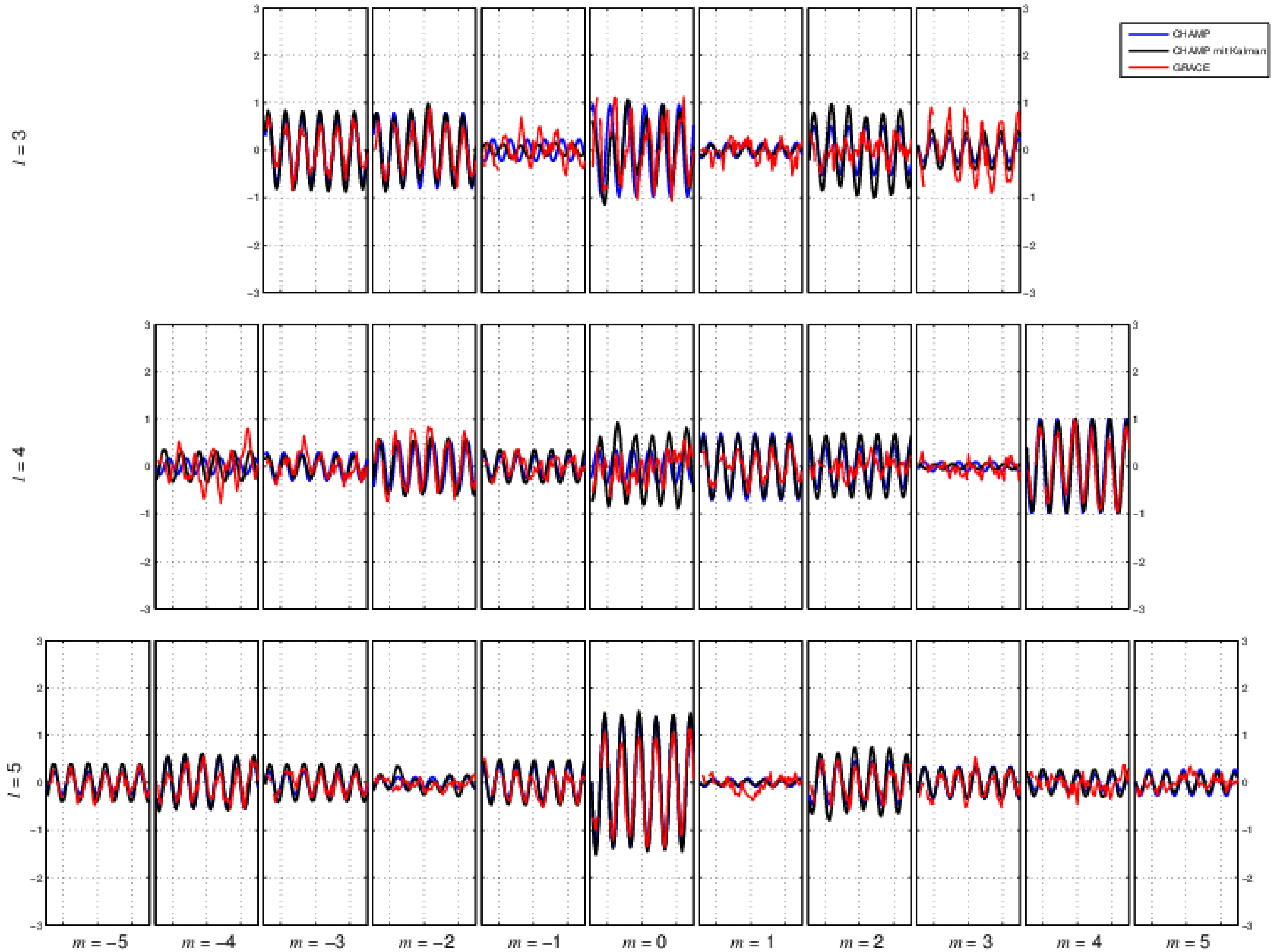

Kalman Filter Monatslösungen

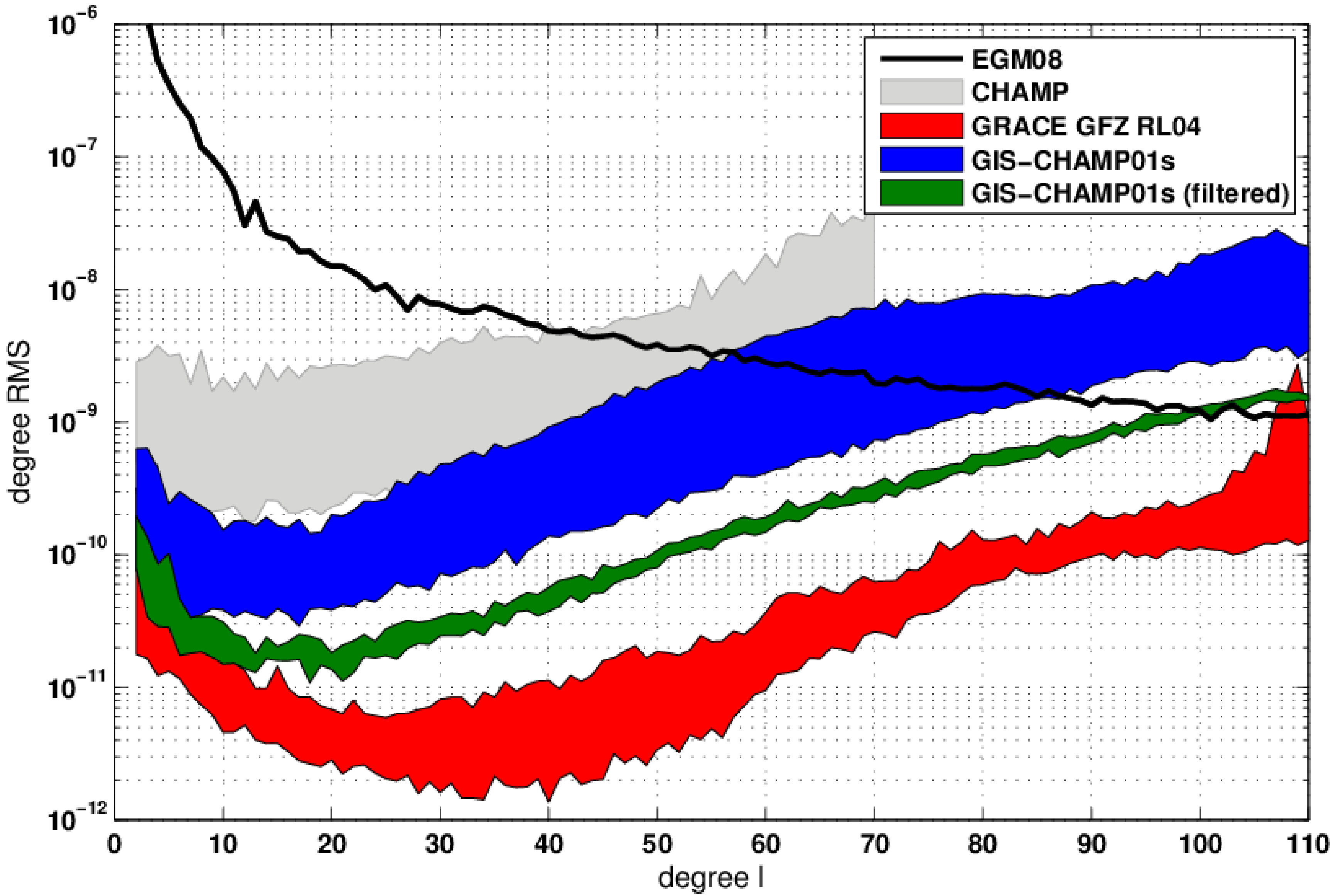

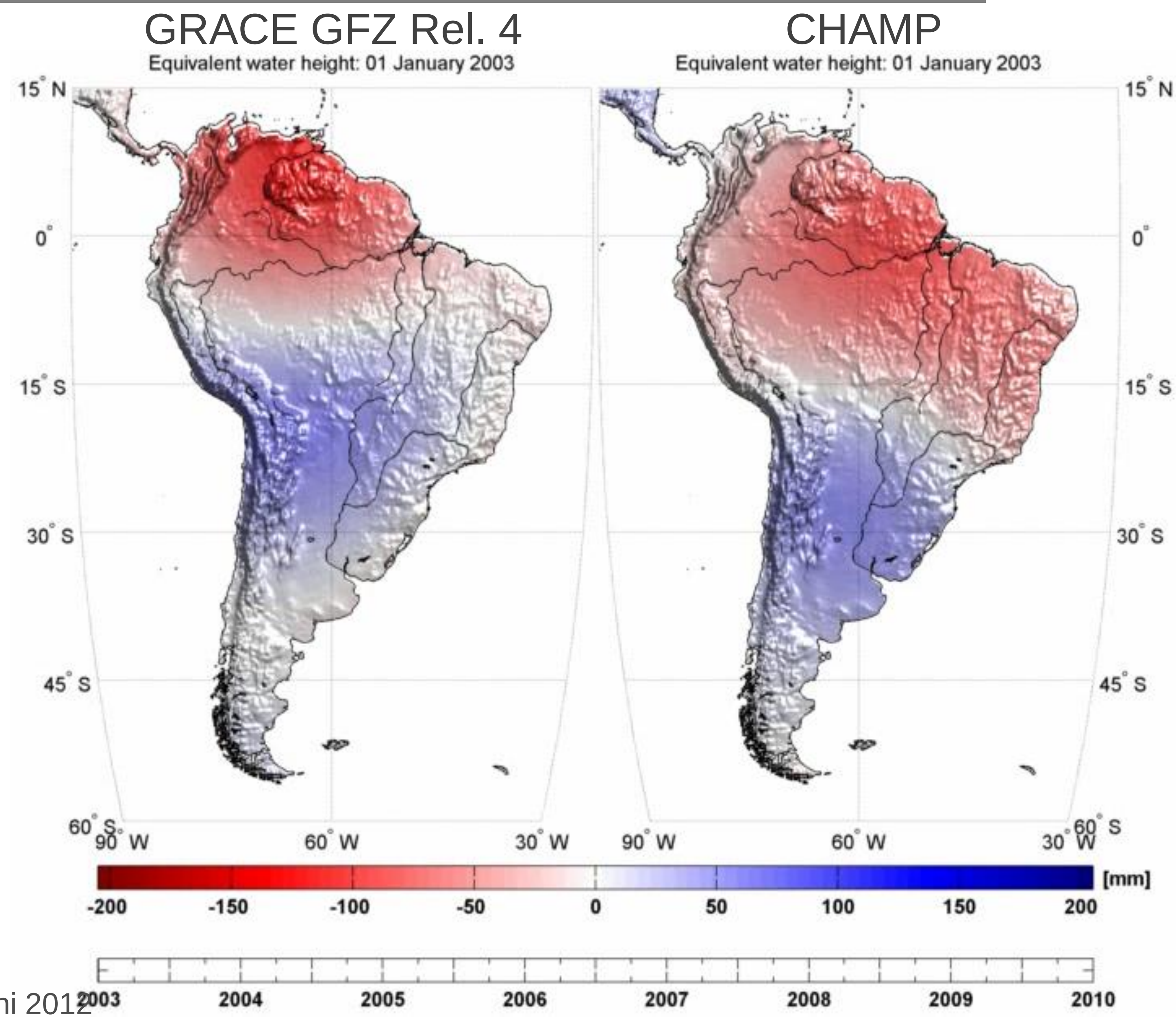
GRACE GFZ Rel. 4
Equivalent water height: 01 January 2003
CHAMP
Equivalent water height: 01 January 2003
15° N
0°
15° S
30° S
45° S
60° S
90° W
60° W
30° W
[mm]
-200
-150
-100
-50
0
50
100
150
200
2003
2004
2005
2006
2007
2008
2009
2010

Zeitreihen

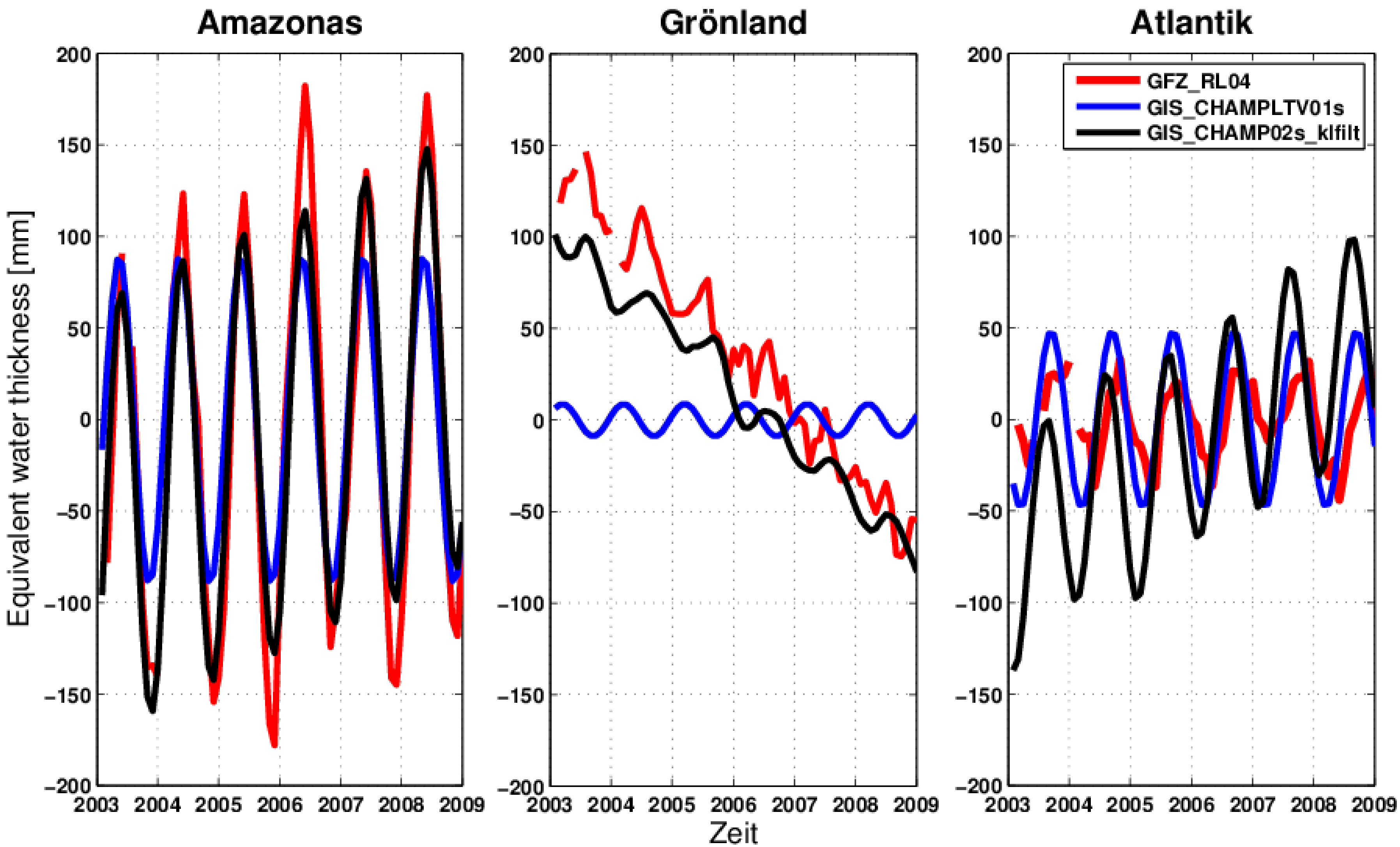
Amazonas
Grönland
Atlantik
Equivalent water thickness [mm]
Zeit
200
150
100
50
0
−50
−100
−150
−200
2003 2004 2005 2006 2007 2008 2009
GFZ_RL04
GIS_CHAMPLTV01s
GIS_CHAMP02s_klfilt

GRACE GFZ Rel. 4 | CHAMP

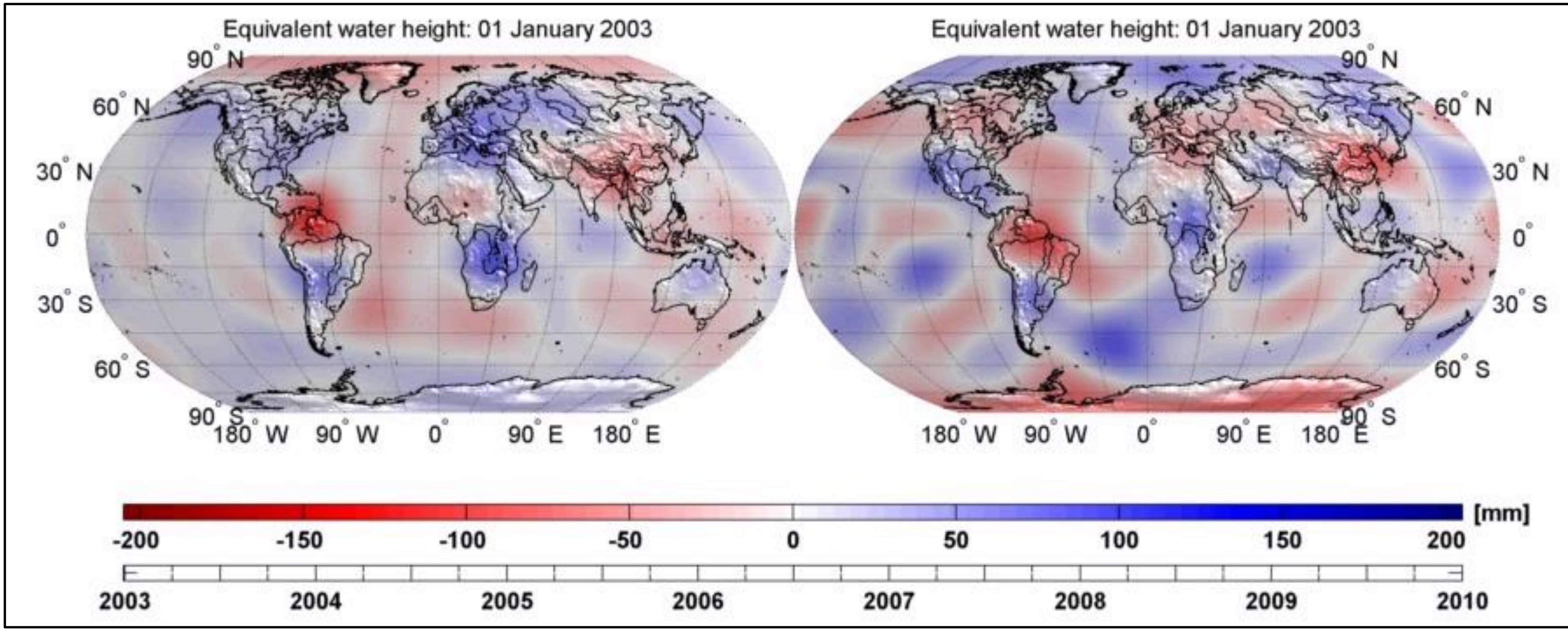

Zusammenfassung

- Verbesserte Monatslösungen aus CHAMP aufgrund von reprozessierten GPS-Daten
- zeitvariables Schweresignal sichtbar
- geringere Qualität gegenüber einer GRACE Lösung
- High-low Konzept als mögliche Brückentechnologie bis GFO (Swarm, Cosmic, Sentinel, …)
- Multi-Satellitenmission
- weitere Prozessierungsverfeinerungen notwendig/möglich

BACKUP

PART III:
GRACE and GRACE Follow-On

GRACE repeat cycles (2/2)

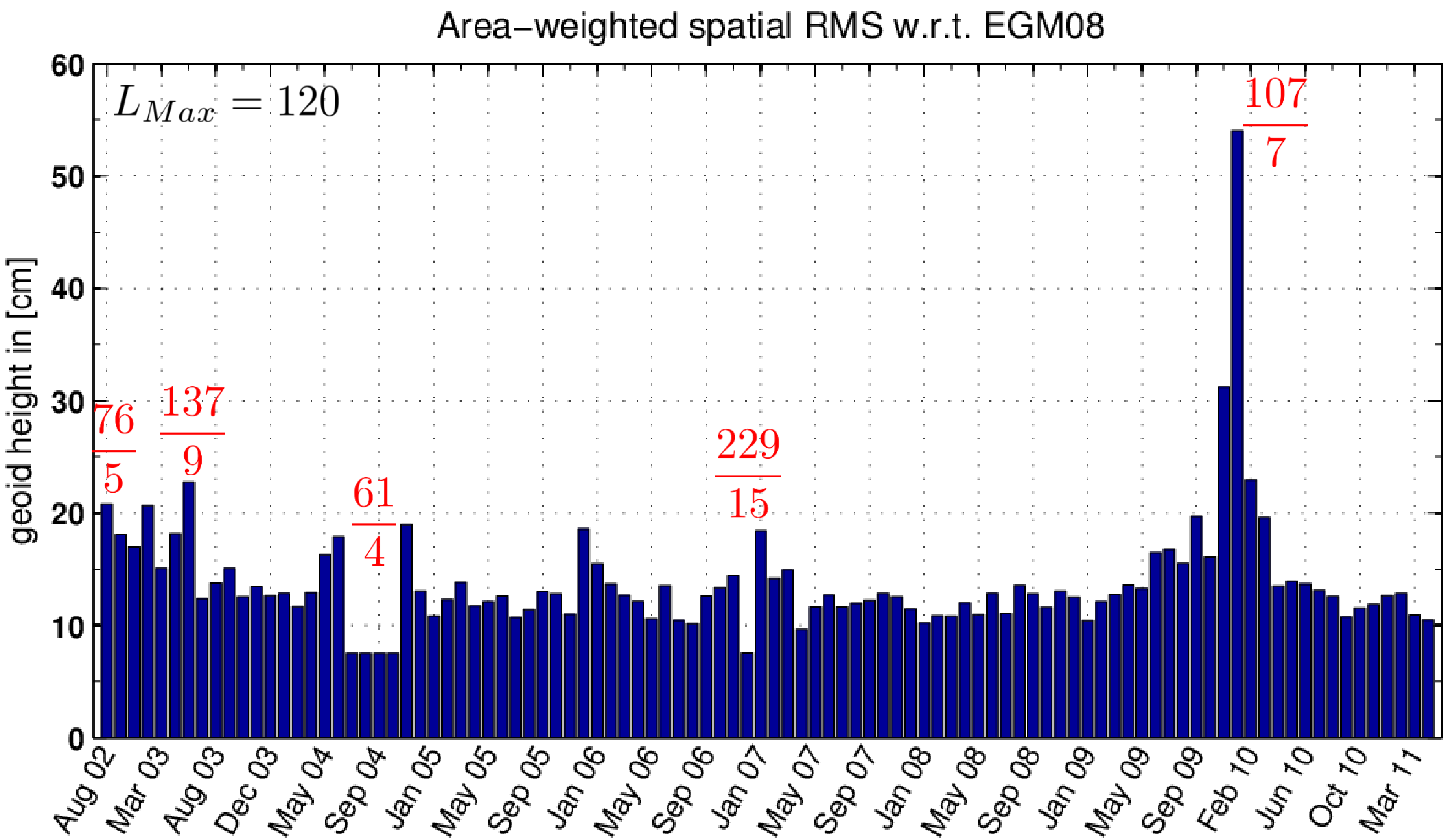

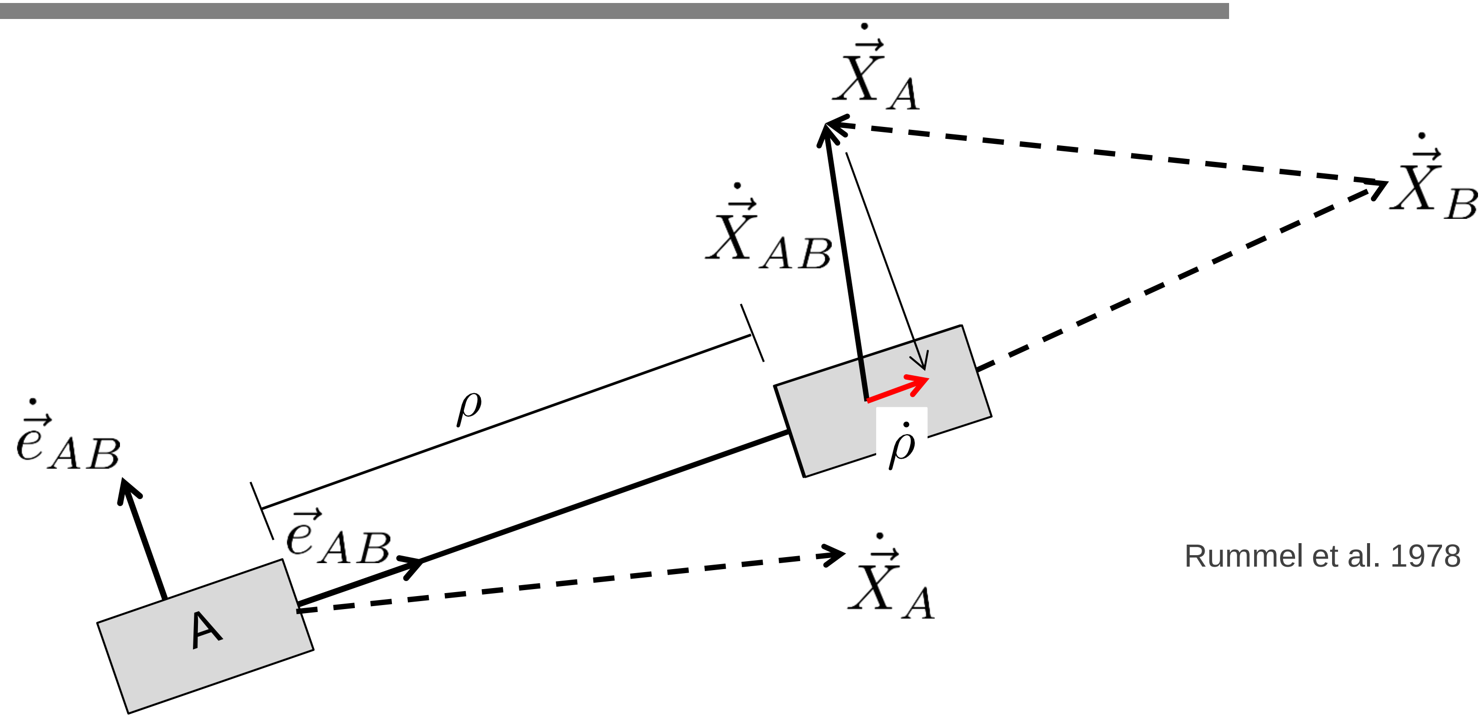

Rummel et al. 1978

Differentiation

Integration

$$\rho = \vec{X}_{AB} \cdot \vec{e}_{AB}$$

$$\dot{\rho} = \dot{\vec{X}}_{AB} \cdot \vec{e}_{AB}$$

$$\ddot{\rho} = \ddot{\vec{X}}_{AB} \cdot \vec{e}_{AB} + \dot{\vec{X}}_{AB} \cdot \dot{\vec{e}}_{AB}$$

$$= \nabla V_{AB}$$

SOLUTION STRATEGIES

Solution strategies

Variational equations

$\rho, \dot{\rho}$ *Classical*
(Reigber 1989, Tapley 2004)

$\rho, \dot{\rho}, \Delta\rho$ *Celestial mechanics approach*
(Beutler et al. 2010, Jäggi 2007)

$\rho, \dot{\rho}$ Short-arc method
(Mayer-Gürr 2006)

...

In-situ observations

Energy Integral $\dot{\rho}$
(Han 2003, Ramillien et al. 2010)

Differential gravimetry $\ddot{\rho}$
(Liu 2010)

LoS Gradiometry $\frac{\ddot{\rho}}{\rho}$
(Keller and Sharifi 2005)

...

Motivation for in-situ observations: local modeling

- Boundary element method

$$V = \int_{\Omega} \frac{\sigma\left(\vec{X}_Q\right)}{\|\vec{X} - \vec{X}_Q\|} d\vec{X}_Q = \sum_{i=1}^{N} \sigma_i \int_{\Omega_i} \frac{\Phi_i}{\|\vec{X} - \vec{X}_Q\|} d\Omega_i$$

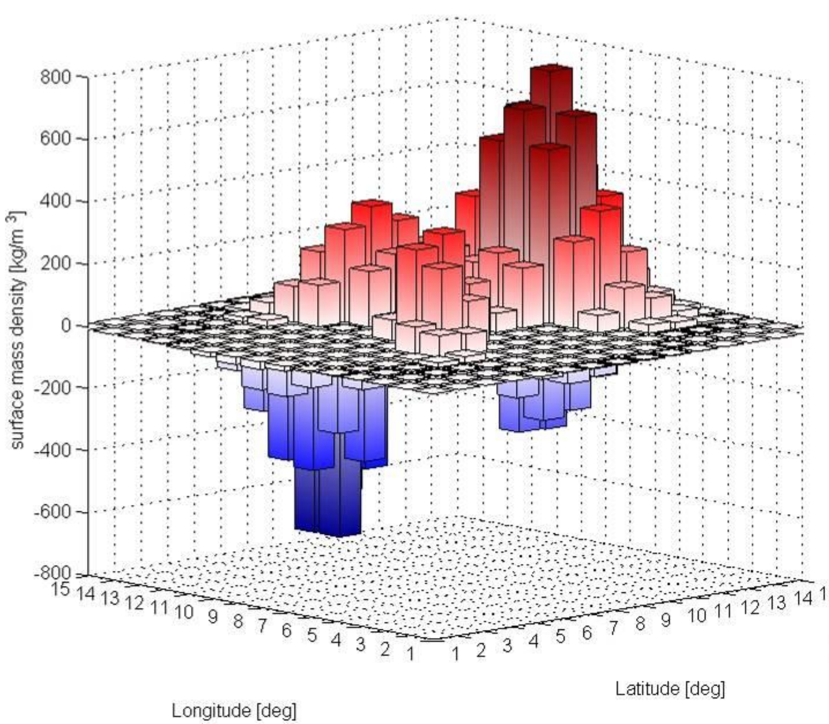

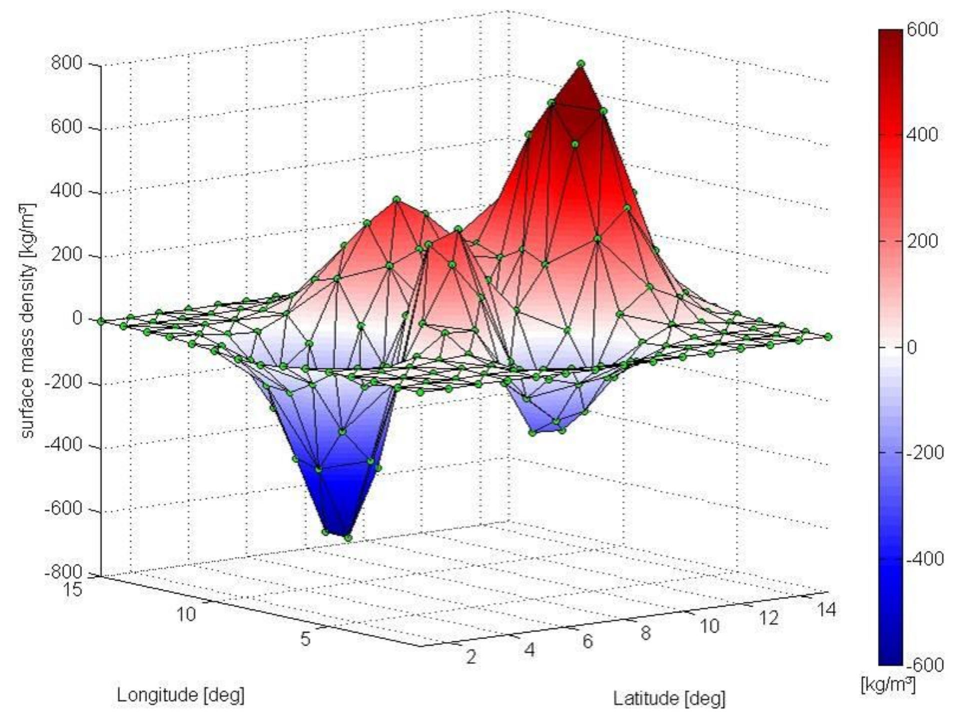

Water problems can only be solved on a basin scale.

(Robert Kandel – Water from Heaven)

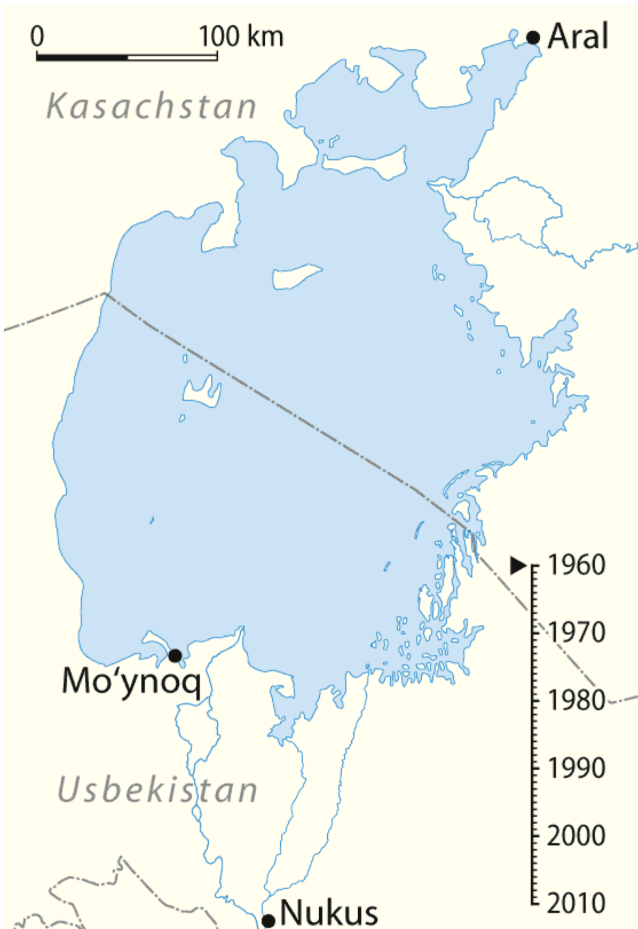

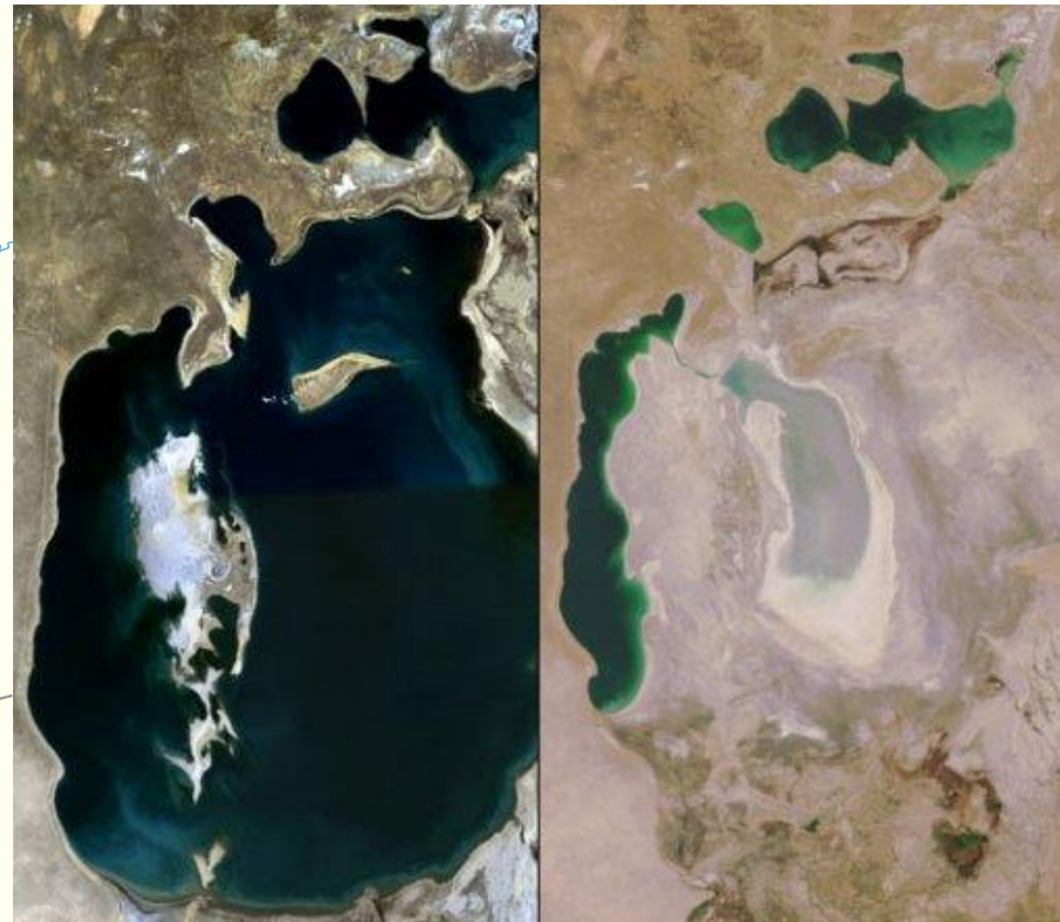

July - September, 1989

October 5, 2008

IN-SITU OBSERVATIONS:
DIFFERENTIAL GRAVITMETRY APPROACH

Instantaneous relative reference frame

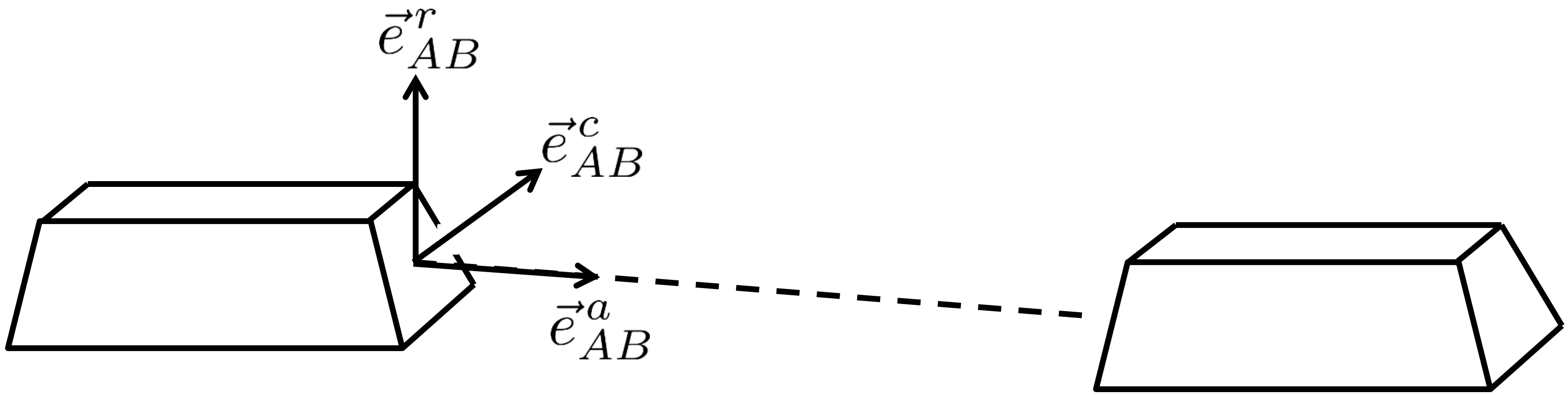

Velocity

Position

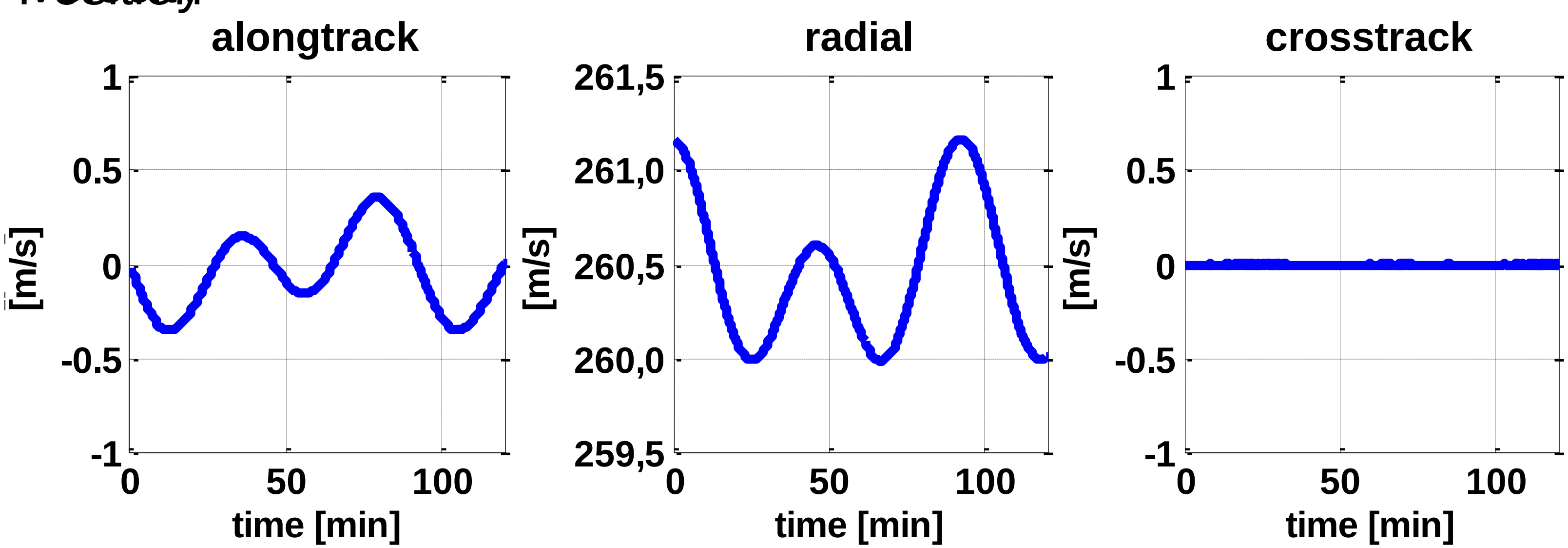

In-situ observation

Range observables:

$$\vec{X}_{AB} = \rho \cdot \vec{e}^{\,a}_{AB}$$

$$\dot{\vec{X}}_{AB} = \dot{\rho} \cdot \vec{e}^{\,a}_{AB} + \rho \cdot \dot{\vec{e}}^{\,a}_{AB}$$

$$\ddot{\vec{X}}_{AB} = \ddot{\rho} \cdot \vec{e}^{\,a}_{AB} + 2 \cdot \dot{\rho} \cdot \dot{\vec{e}}^{\,a}_{AB} + \rho \cdot \ddot{\vec{e}}^{\,a}_{AB}$$

Multiplication with unit vectors:

GRACE

$$\ddot{\vec{X}}_{AB} \cdot \vec{e}^{\,a}_{AB} = \ddot{\rho} \quad + \quad 0 \quad + \quad \rho \cdot \ddot{\vec{e}}^{\,a}_{AB} \cdot \vec{e}^{\,a}_{AB}$$

$$\ddot{\vec{X}}_{AB} \cdot \vec{e}^{\,r}_{AB} = 0 \quad + \quad 2 \cdot \dot{\rho} \cdot \|\dot{\vec{e}}^{\,a}_{AB}\| \quad + \quad \rho \cdot \ddot{\vec{e}}^{\,a}_{AB} \cdot \vec{e}^{\,r}_{AB}$$

$$\ddot{\vec{X}}_{AB} \cdot \vec{e}^{\,c}_{AB} = 0 \quad + \quad 0 \quad + \quad \rho \cdot \ddot{\vec{e}}^{\,a}_{AB} \cdot \vec{e}^{\,c}_{AB}$$

Relative motion

absolute motion neglected!

$$\ddot{\vec{X}}_{AB} \cdot \vec{e}^{a}_{AB} = \ddot{\rho} + \rho \cdot \ddot{\vec{e}}^{a}_{AB} \cdot \vec{e}^{a}_{AB}$$

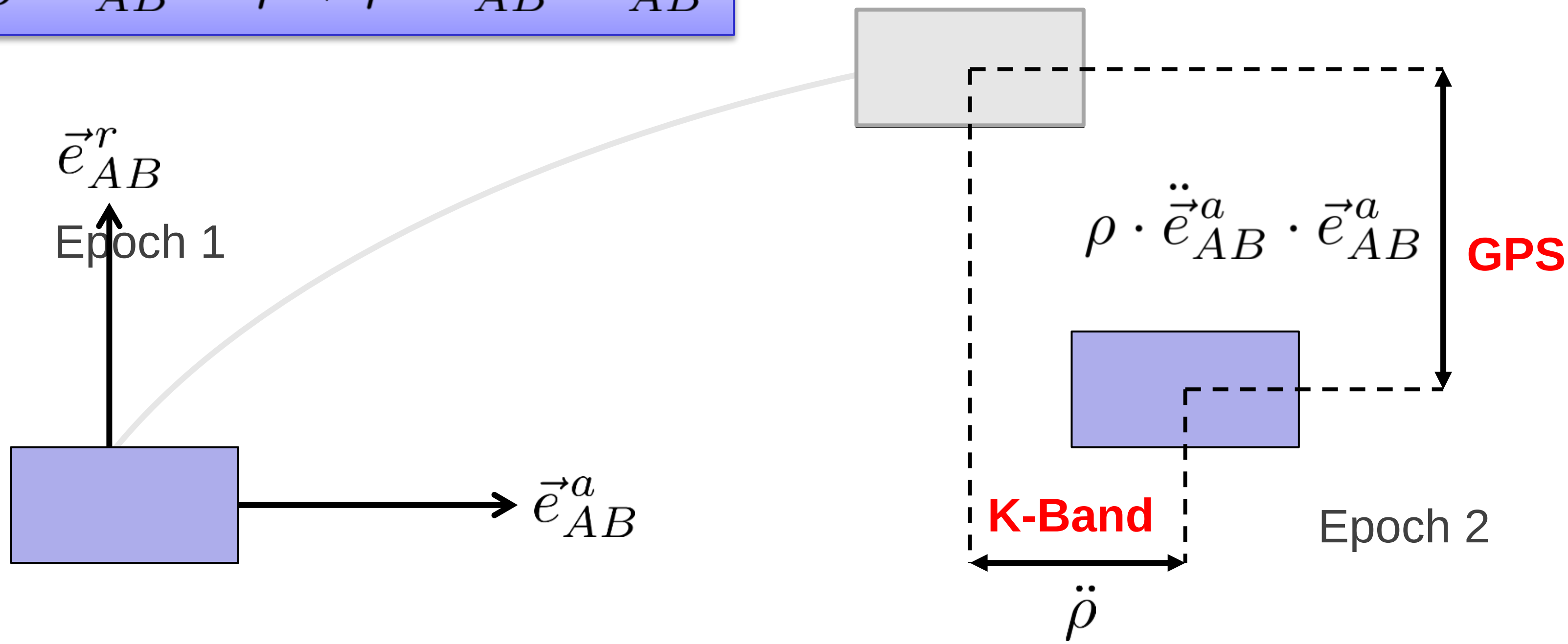

$$\begin{aligned}
\rho \cdot \ddot{\vec{e}}^{a}_{AB} \cdot \vec{e}_{AB} &= \vec{X}_{AB} \cdot \ddot{\vec{e}}^{a}_{AB} &&= -\dot{\vec{X}}_{AB} \cdot \dot{\vec{e}}^{a}_{AB} \\
&= -\dot{\rho} \cdot \|\dot{\vec{e}}^{a}_{AB}\|^2 &&= -\frac{1}{\rho}\left(\dot{\vec{X}}_{AB} \cdot \dot{\vec{X}}_{AB} - \dot{\rho}^2\right) \\
&= -\rho \cdot \omega_c^2
\end{aligned}$$

Limitation

Combination of highly precise K-Band observations with comparably low accurate GPS relative velocity

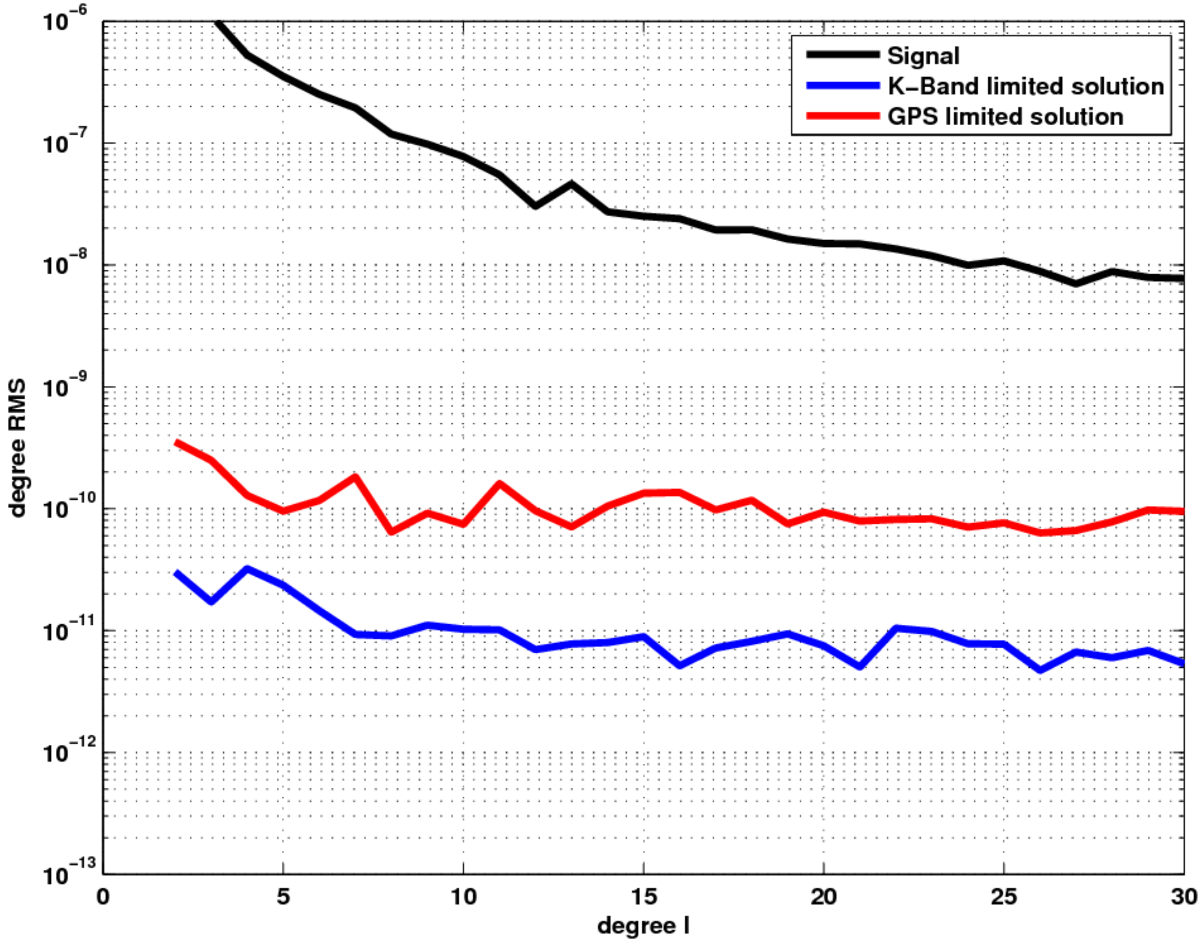

Residual quantities

- Orbit fitting using the homogeneous solution of the variational equation with a known a priori gravity field

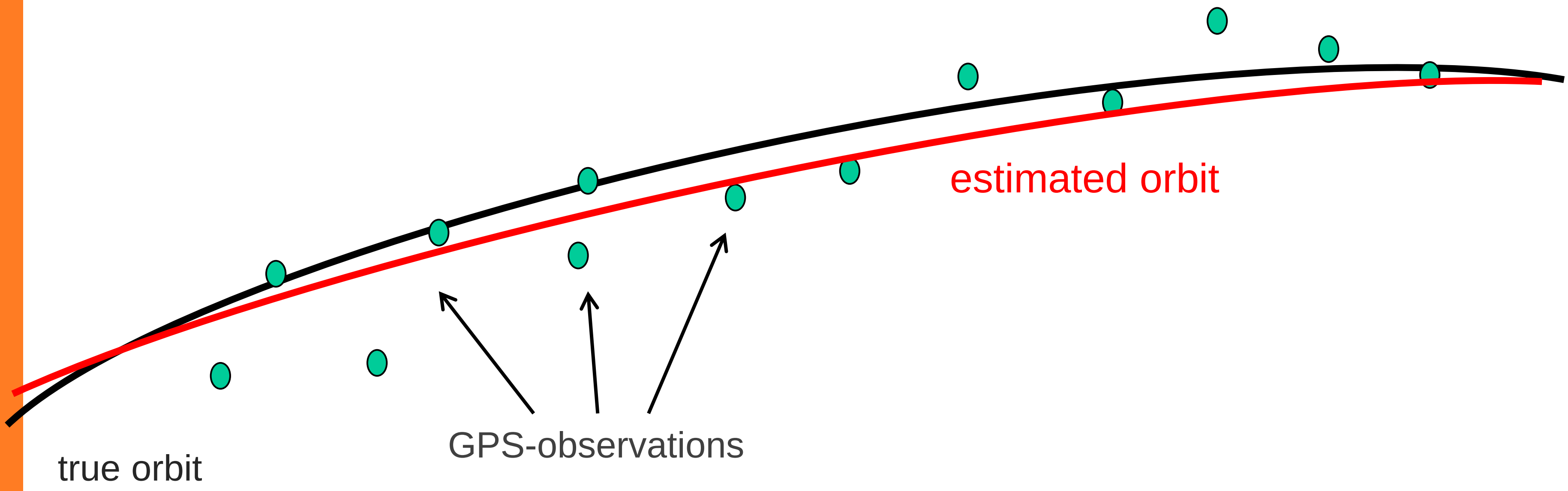

- Avoiding the estimation of empirical parameters by using short arcs

Residual quantities

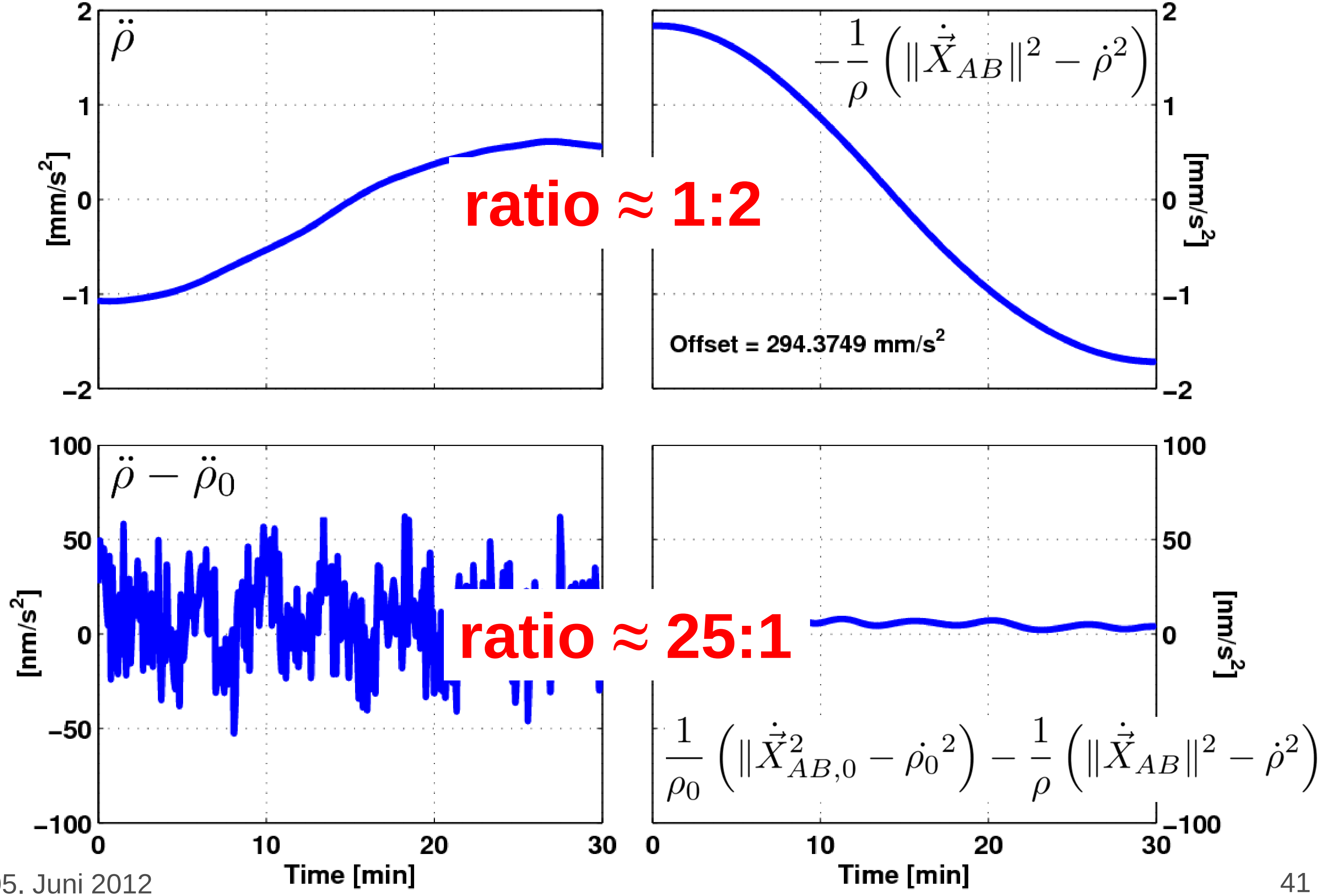

Approximated solution

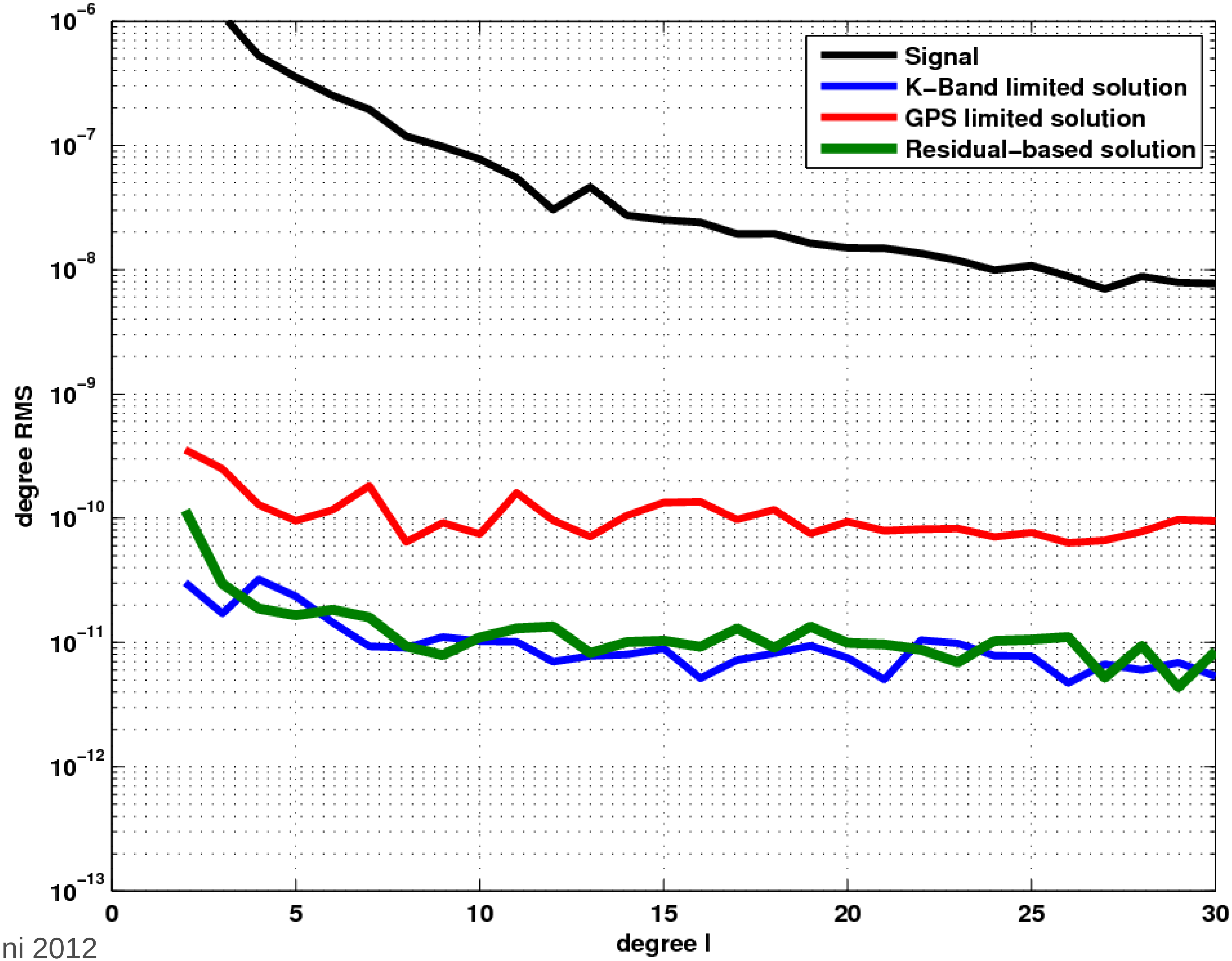

GRACE FOLLOW-ON

Next generation GRACE

- New type of inter-satellite distance measurement based on laser interferometry
- Noise reduction by factor 10 expected (factor 1000 possible)

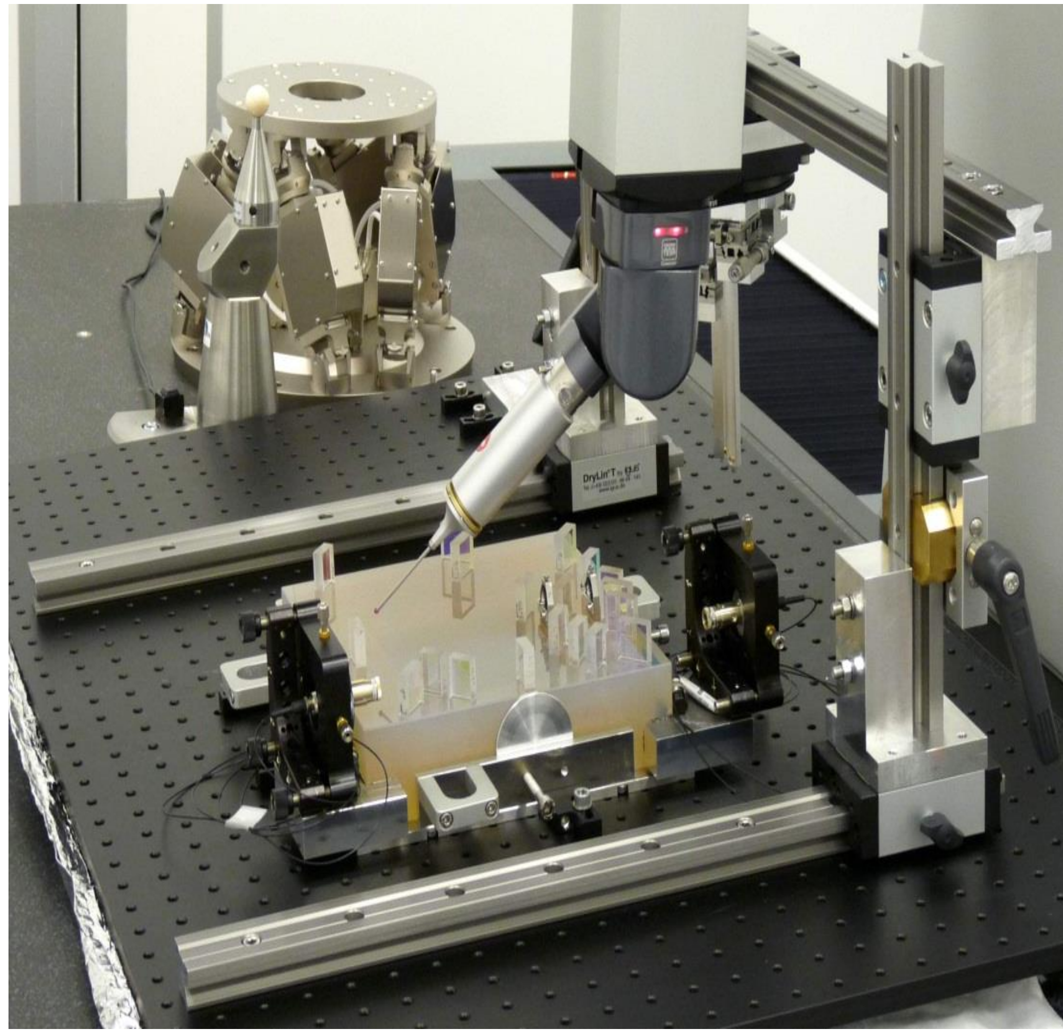

M. Dehne, Quest

Solution for next generation GRACE

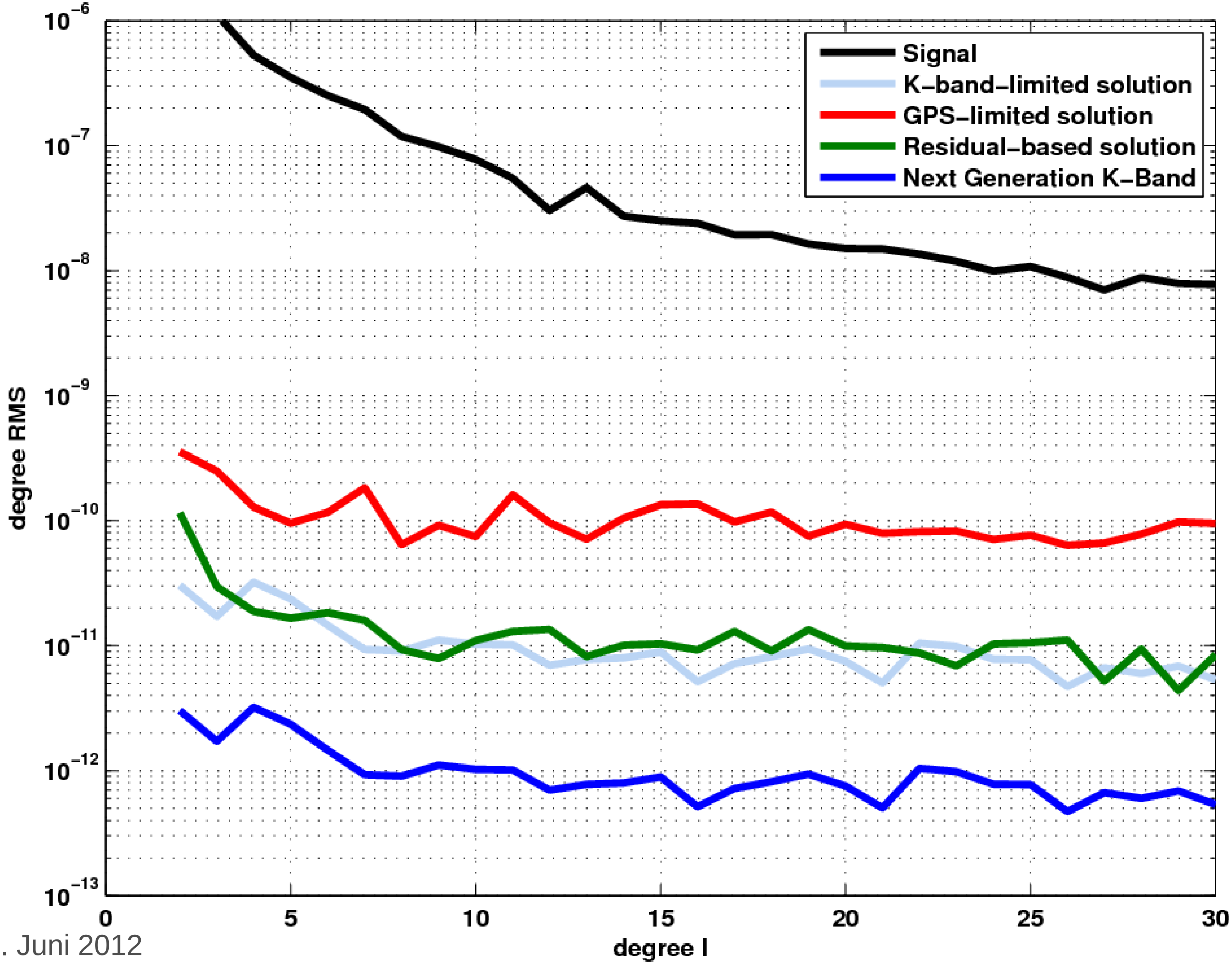

Variational equations for velocity term

- Reduction to residual quantity insufficient
- Modeling the velocity term by variational equations:

$$f = -\frac{1}{\rho}\left(\|\dot{\vec{X}}_{AB}\|^2 - \dot{\rho}^2\right)$$

$$\frac{\partial f}{\partial p_i} = \frac{\partial f}{\partial x_A}\frac{\partial x_A}{\partial p_i} + \frac{\partial f}{\partial x_B}\frac{\partial x_B}{\partial p_i} + \dots\dots\dots + \frac{\partial f}{\partial \dot{z}_B}\frac{\partial \dot{z}_B}{\partial p_i}$$

- Application of the method of the variations of the constants
- Alternatively: application of the Hill equations

Results

- only minor improvements
- possibly the orbit fit to the GPS positions as a limiting factor

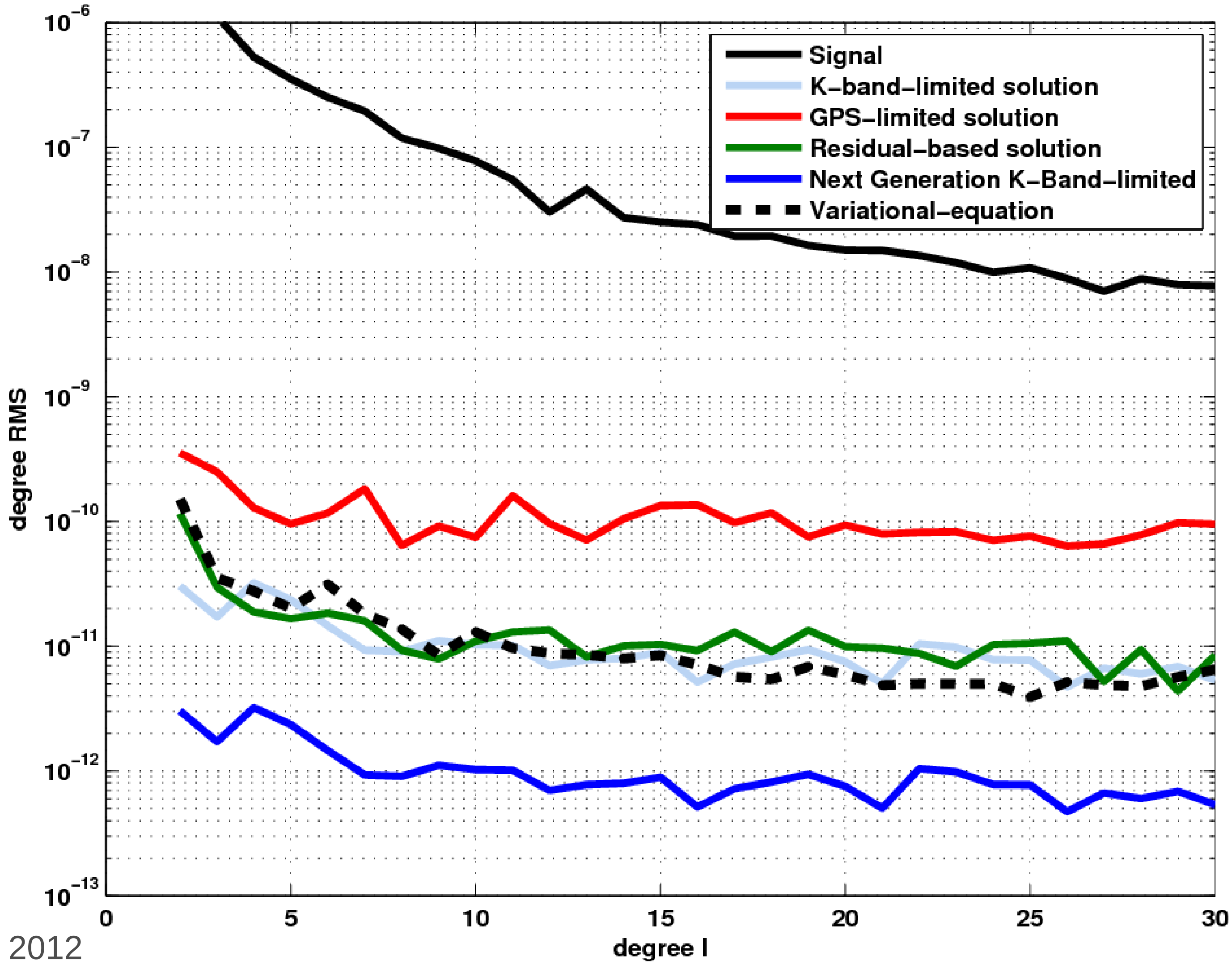

ICCT

Applicability of current GRACE solution strategies to the next generation of inter-satellite range observations

Chair: Matthias Weigelt

Co-Chair: Adrian Jäggi

Objectives

The objectives of the study group are to:

- *investigate each solution strategy, identify approximations and linearizations and test them for their permissibility to the next generation of inter-satellite range observations,*
- *i ... e*
  n

It is <u>not</u> the idea,
to find the best approach!

- *q ... al*
  force modeling,
- *investigate the interaction with global and local modeling,*
- *extend the applicability to planetary satellite mission, e.g. GRAIL*
- *establish a platform for the discussion and in-depth understanding of each approach and provide documentation.*

Example: sensitivity to non-gravitational error sources

- Calibration of the accelerometer:
  - Calibration model for GRACE:

$$\tilde{\vec{f}} = (1 + S_1)\,\vec{f} + \vec{b}$$

  - Full calibration model for an accelerometer

$$\tilde{\vec{f}} = (1 + S_1)\,\vec{f} + S_2\vec{f}^{\,2} + N\vec{f} + \vec{b}$$

with: $\vec{b}$ bias

S_1 linear scale matrix

S_2 non-linear scale matrix

N misalignment matrix

- Calibration with GPS-positioning!

Decomposition of the surface into elements with finite extend (boundary elements)

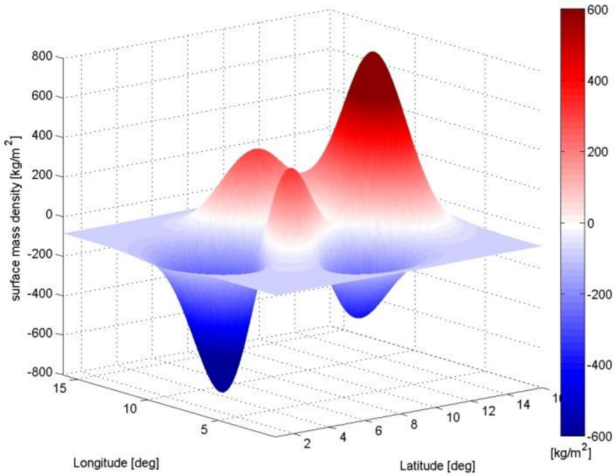

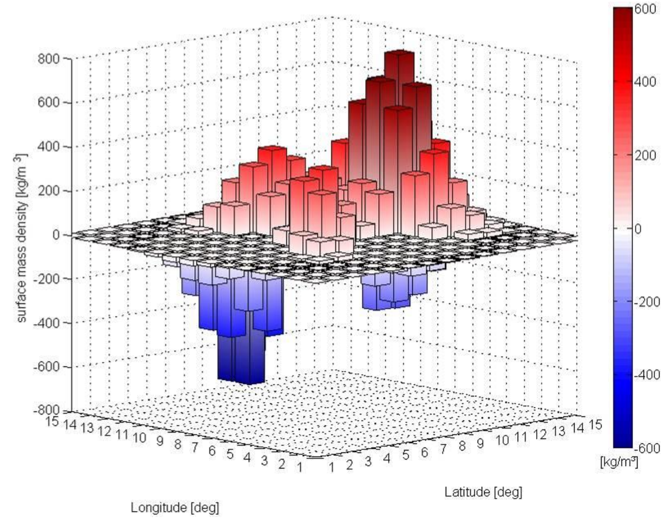

e.g. blocks

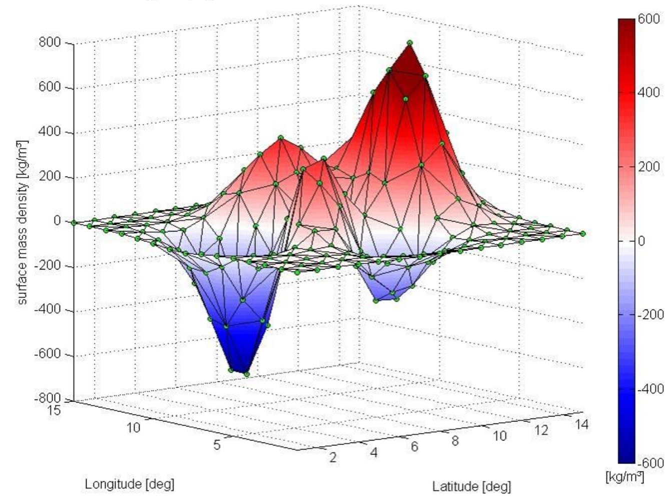

e.g. triangles

Example: Consider the single layer potential

$$V = \int_{\Omega} \frac{\sigma\left(\vec{X}_Q\right)}{\|\vec{X} - \vec{X}_Q\|} d\vec{X}_Q$$

Separation of the surface into elements: $\Omega = \sum_{i=1}^{N} \Omega_i$

Assumption:

$$\vec{X} = \sum_{k=1}^{K} \Phi_{i,k}^{\vec{X}} \vec{X}_{i,k}$$

$$\sigma_i\left(\vec{X}_Q\right) = \sum_{k=1}^{K} \Phi_{i,k}^{\sigma} \sigma_{i,k}\left(\vec{X}_{i,k}\right)$$

The boundary elements are called ***isoparametric*** *if* $\Phi_{i,k}^{\vec{X}} = \Phi_{i,k}^{\sigma}$

Basic principle

Example: Consider the single layer potential

Including transformation to the normal triangle and spherical integration

$$V = \frac{GR^2}{4\pi} \sum_{i=1}^{N} \sum_{k=1}^{K} \sigma_{i,k} \int_{-1}^{1} \int_{-1}^{-\xi} \frac{J_i(\xi,\eta) \cdot \Phi_{i,k}(\xi,\eta) \cdot \cos\phi(\xi,\eta)}{\|\vec{X}(r,\phi,\lambda) - \vec{X}(R,\phi(\xi,\eta),\lambda(\xi,\eta))\|} d\eta d\xi$$

Integration by Gaussian quadrature

$$\int_{-1}^{1} \int_{-1}^{-\xi} \ldots d\eta d\xi \Rightarrow \sum_{l=1}^{L} \sum_{m=1}^{L} w_l w_m \ldots \qquad \text{with } w_l w_m = 0 \text{ for } m > l$$

Integration is exact for a polynomial of order 2L.

Base functions are

- *strictly space-limited (i.e. band-unlimited)*
- *compact*
- *continuous but not differentiable at the edges*
- *singular if the point of interest lies inside or on the corner of the element*
  - *Weak singularity for potential* $\left(\frac{1}{r}\right)$
  - *Strong singularity for gradient* $\left(\frac{1}{r^3}\right)$

In collaboration with JSG 0.3:

Comparison of methodologies for regional gravity field modeling

Chair: M. Schmidt, Co-Chair: Ch. Gerlach

Users interest in **regional mass variations**, e.g. floodings:

Requirements are:

- **enhanced** spatial **resolution**,
- **arbitrary regions** of interests (river basins, etc.),
- **combinations of measurement techniques** (space gravity missions, airborne, terrestrial, altimetry, other remote sensing, etc.).

Example: linear triangle

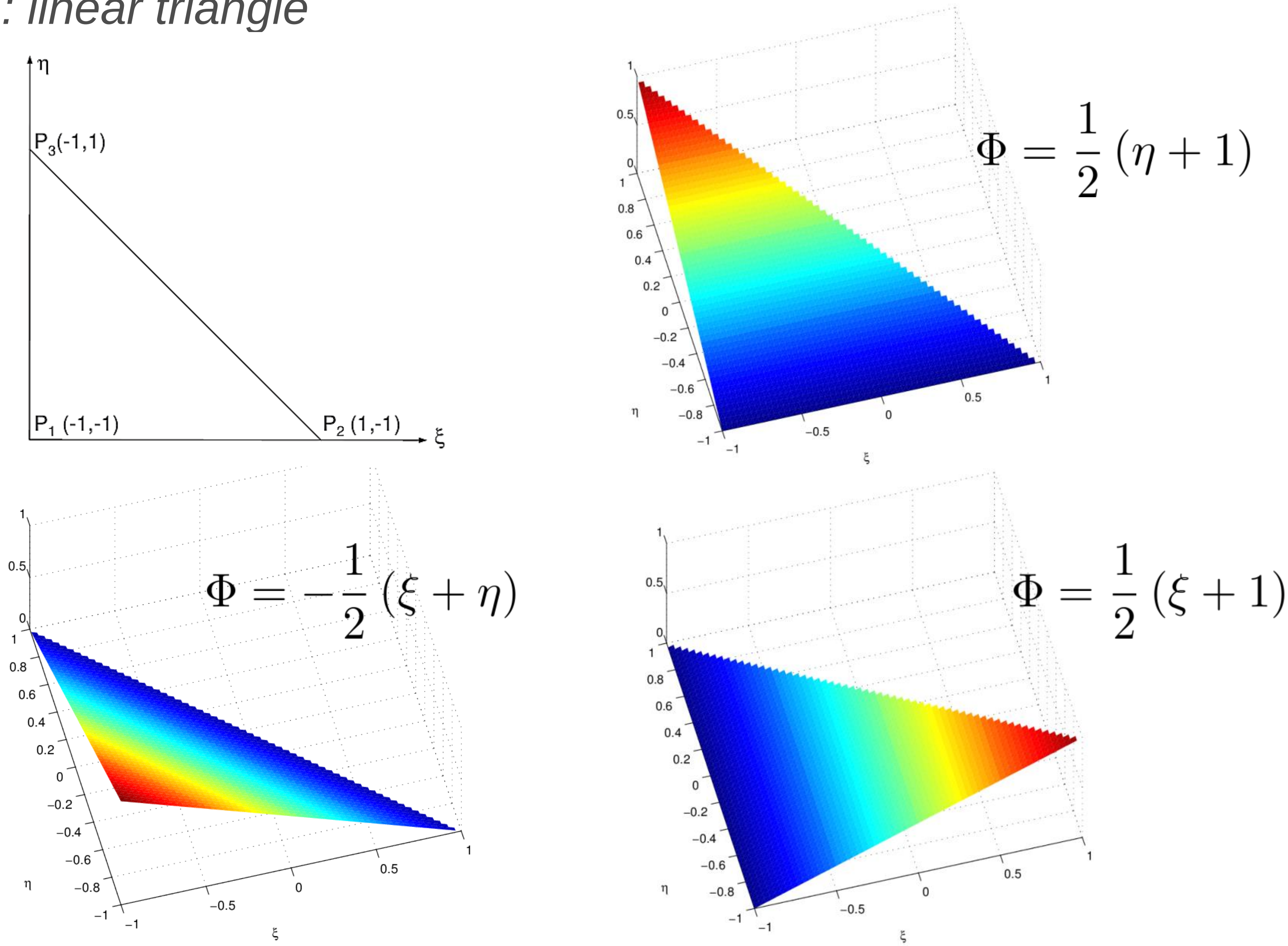

$$\Phi = \frac{1}{2}(\eta + 1)$$

$$\Phi = -\frac{1}{2}(\xi + \eta)$$

$$\Phi = \frac{1}{2}(\xi + 1)$$

Other base functions

six node triangle

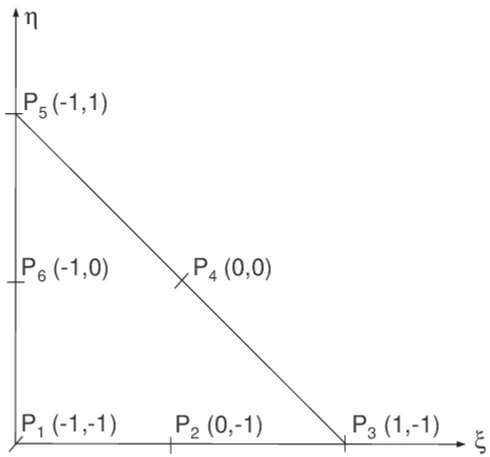

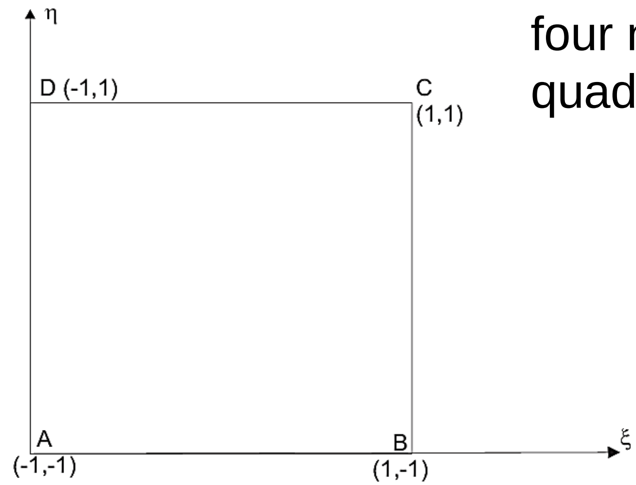

four node quadrilateral

eight node quadrilateral:

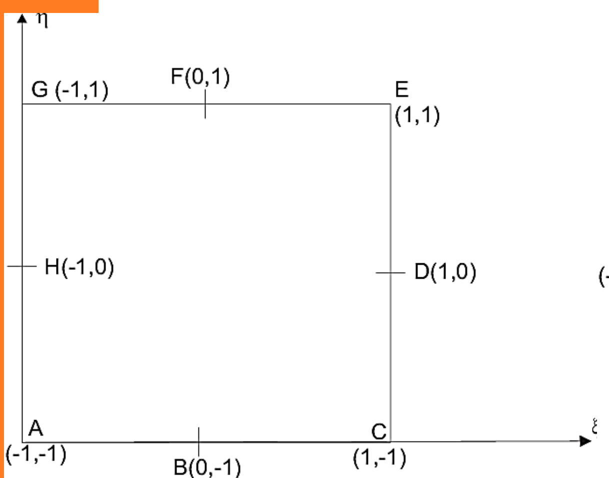

nine node quadrilateral:

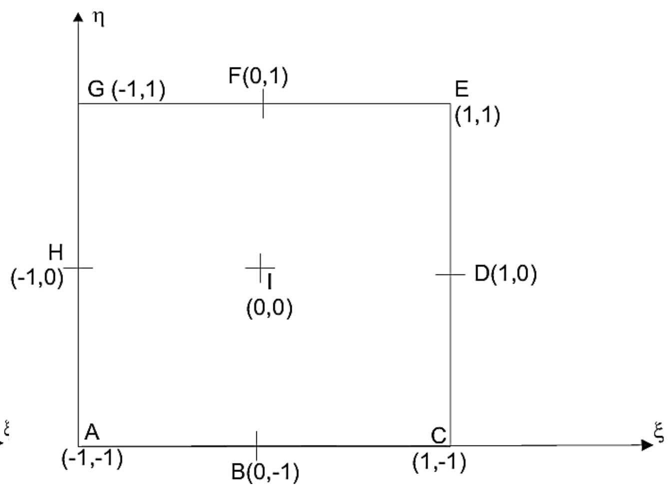

infinite quadrilateral:

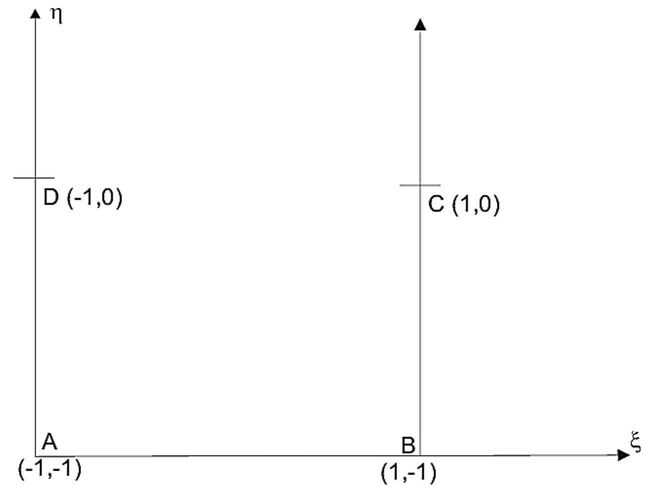

Point Grids

Point grid: any (as long as a proper tessellation is possible)

Currently based on the maxima and minima of an a priori field

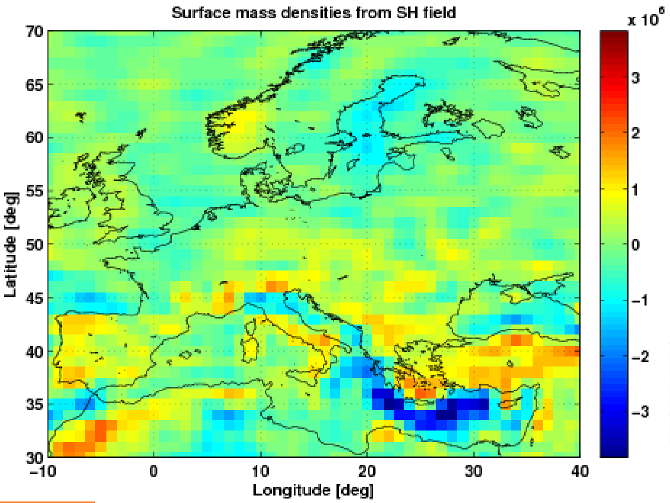

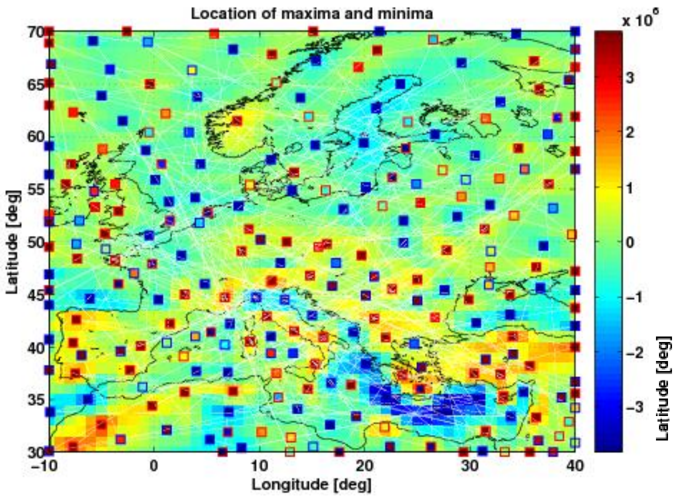

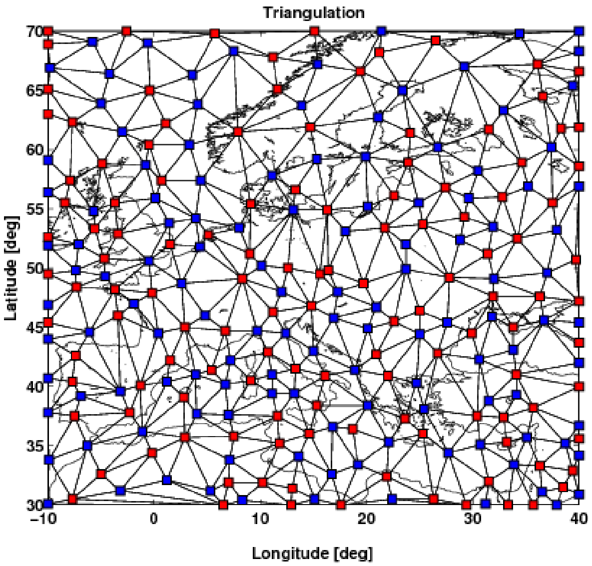

Solution approach

- *Search for maxima and minima of an a priori field*
- *Triangulation by Delaunay tessellation*
- *Least-squares adjustment*
  - *brute-force*
  - *assembly of the normal matrix (singularity!)*
  - *full consideration of the stochastic information*
- *No regularization*
  - *objective: avoid regularization by proper grid*
  - *iterative search for vertices*

Closed loop simulation: noisefree and h=0km

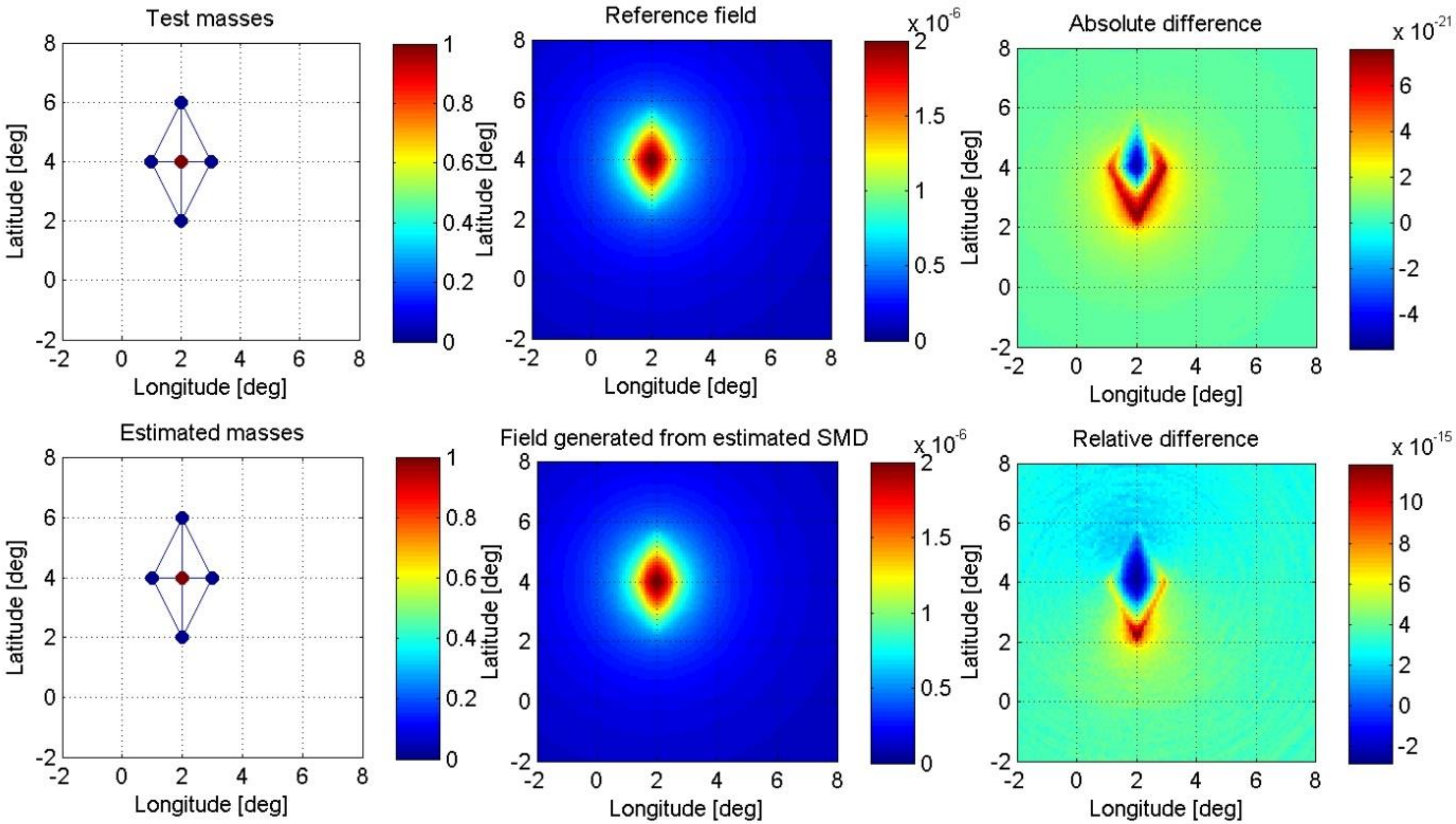

Closed loop simulation: noise=1% and h=400km

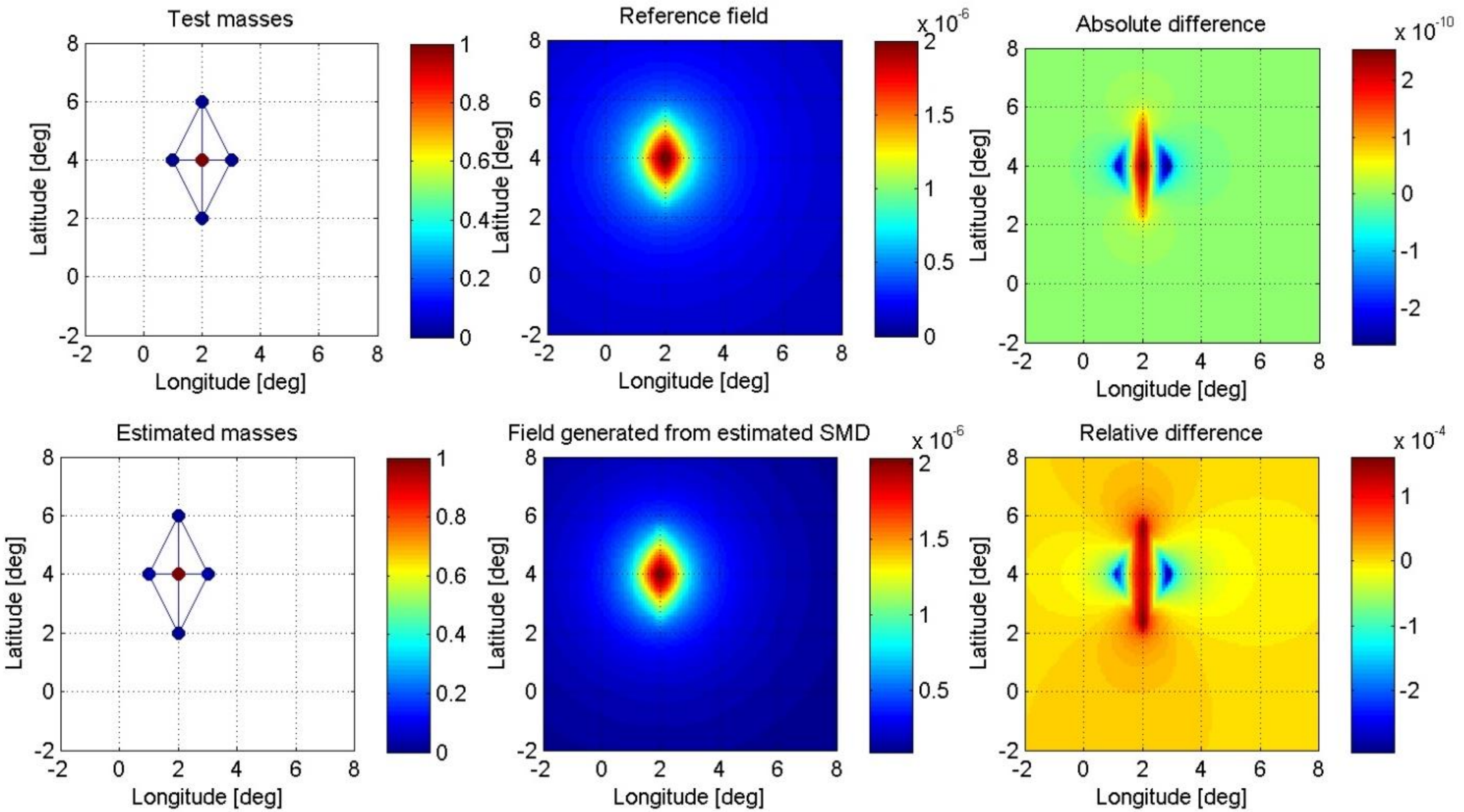

Simulation study